Impact of Mid-T Heat Treatments on the Sensitivity to Trapped Magnetic Flux

J. C. Wolff, J. Eschke, A. Goessel, W. C. A. Hillert, K. Kasprzak, D. Reschke, L. Steder, L. Trelle, M. Wiencek
Cavity Meeting, 04.10.2023

HELMHOLTZ

DESY.

Mid-T Heat Treatments: High Q_0 in Low Field Environment

➢ Increased Sensitivity to Trapped Magnetic Flux S

mid-T heat treatments (~300 °C)

- highest Q_0 of up to $5 \cdot 10^{10}$ at 2 K achieved at FNAL, IHEP, KEK & DESY
- increased sensitivity to trapped magentic flux S observed at FNAL, KEK & DESY

to benefit from mid-T heat treatment:

- minimize B_{trap}
- consequently minimize increase of R_s by R_{flux}

Mid-T Heat Treatments: High Q_0 in Low Field Environment

➢ Increased Sensitivity to Trapped Magnetic Flux S

mid-T heat treatments (~300 °C)

- highest Q_0 of up to $5 \cdot 10^{10}$ at 2 K achieved at FNAL, IHEP, KEK & DESY
- increased sensitivity to trapped magentic flux S observed at FNAL, KEK & DESY

to benefit from mid-T heat treatment:

- minimize B_{trap}
- consequently minimize increase of R_s by R_{flux}

separately study impact on B_{trap} of:

B: 10 µT

- cool down velocity
- spatial temperature gradient

for assumed technical extrema

QE performance

- evaluate R_s
- approximate R_{flux} by baseline curve (0 µT)
- calculate $S = R_{flux} / B_{trap}$

Mid-T Heat Treatments: High Q_0 in Low Field Environment

➢ Increased Sensitivity to Trapped Magnetic Flux S

mid-T heat treatments (~300 °C)

- highest Q_0 of up to $5 \cdot 10^{10}$ at 2 K achieved at FNAL, IHEP, KEK & DESY
- increased sensitivity to trapped magentic flux S observed at FNAL, KEK & DESY

to benefit from mid-T heat treatment:

- minimize B_{trap}
- consequently minimize increase of R_s by R_{flux}

separately study impact on B_{trap} of:

B: 10 µT

- cool down velocity
- spatial temperature gradient

for assumed technical extrema

QE performance

- evaluate R_s
- approximate R_{flux} by baseline curve (0 µT)
- calculate $S = R_{flux} / B_{trap}$

test series

1DE03 fine grain

bef. mid-T

1DE09 fine grain

aft. mid-T

1DE26 large grain

bef. mid-T | aft. mid-T

Spatial Dependency of Flux Expulsion Expected

➢ Magnetometric Mapping System used to Study Magnetic Flux Expulsion Behavior

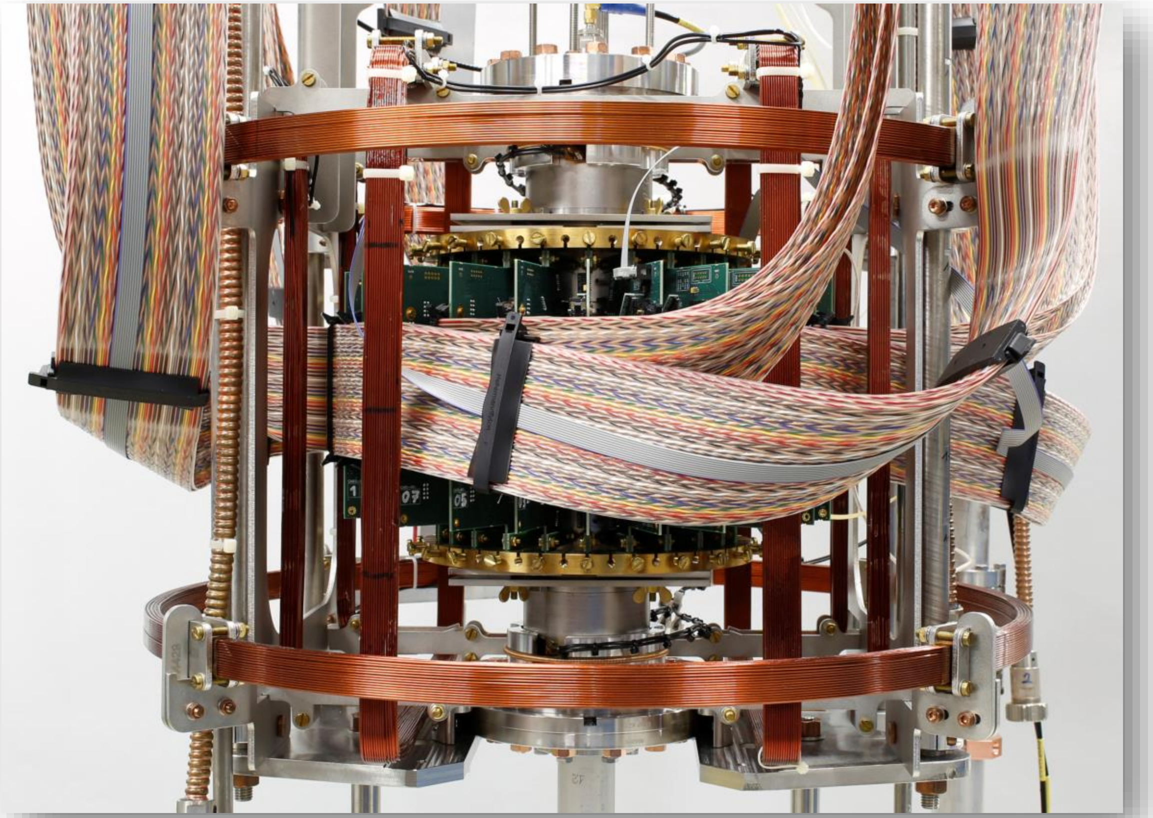

based on first magnetometric mapping approach
at HZB [B. Schmitz et al., F. Kramer et al.]

system consists of:

23 sensor boards

- ➢ 27 single axis sensors
- ➢ arranged in groups of three
- ➢ 9 sensor groups

1 thermocouple board

- ➢ Temp 1: upper iris
- ➢ Temp 2: equator
- ➢ Temp 3: lower iris

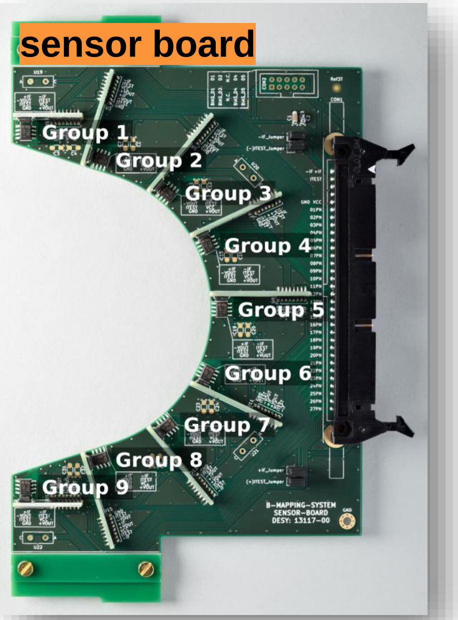

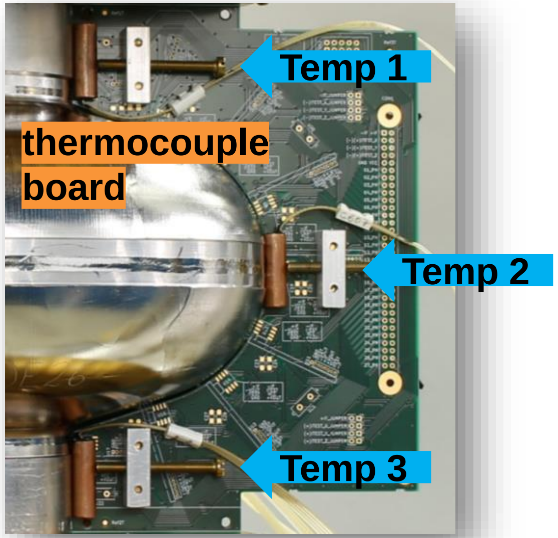

Digitize Sensor Signals Inside of Cryostat

➢ **Avoid High Number of Cable Feed Throughs Through Cryostat Lid**

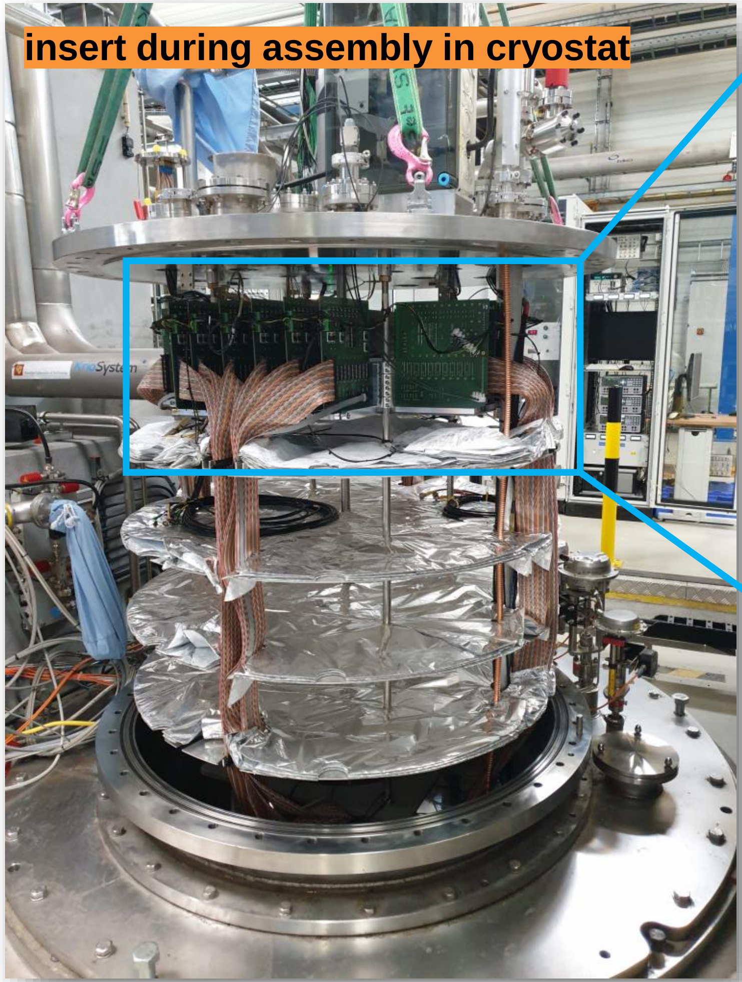

supply- & digital signal lines

PID Controlled Cool Down Velocity

➢ Ensure Test Comprehensive Consistent Conditions

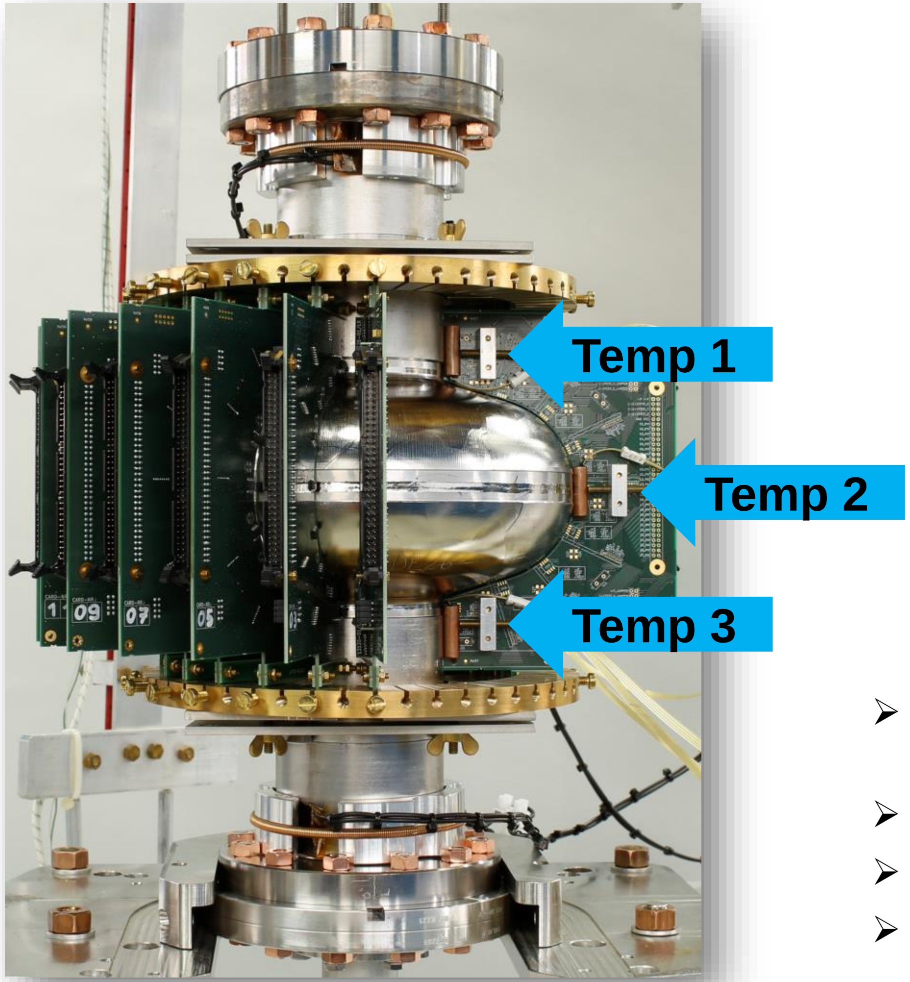

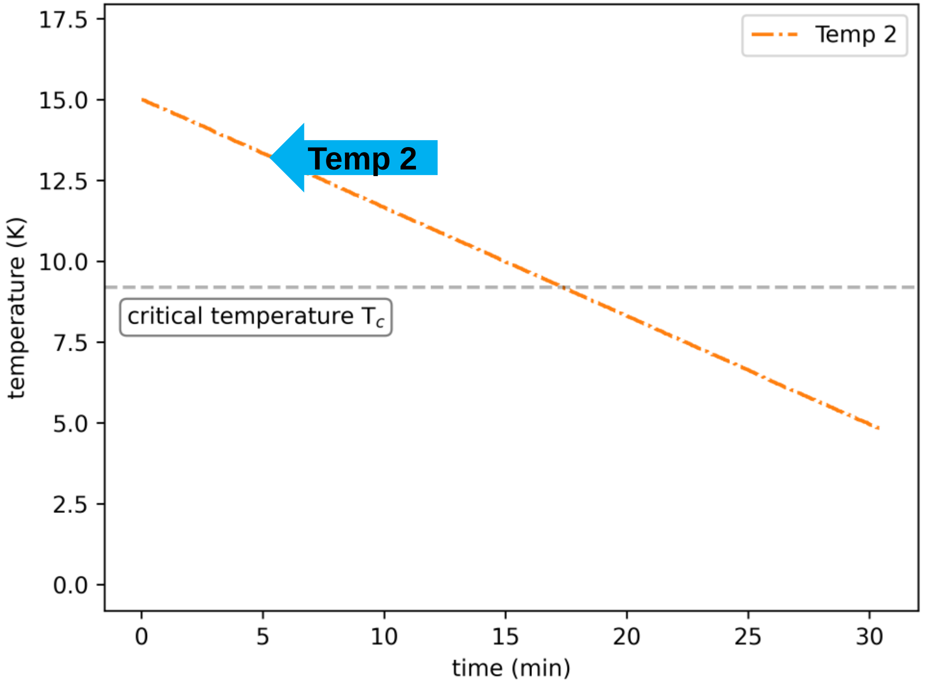

- constant cool down velocity: -5 K/h or -20 K/h
- LHe level lowered below setup
- pressure PID controlled reduced
- equator thermocouple Temp 2 used as reference

PID Controlled Spatial Temperature Gradient

➢ Suppress Stray Impact of a Changed Cool Down Velocity

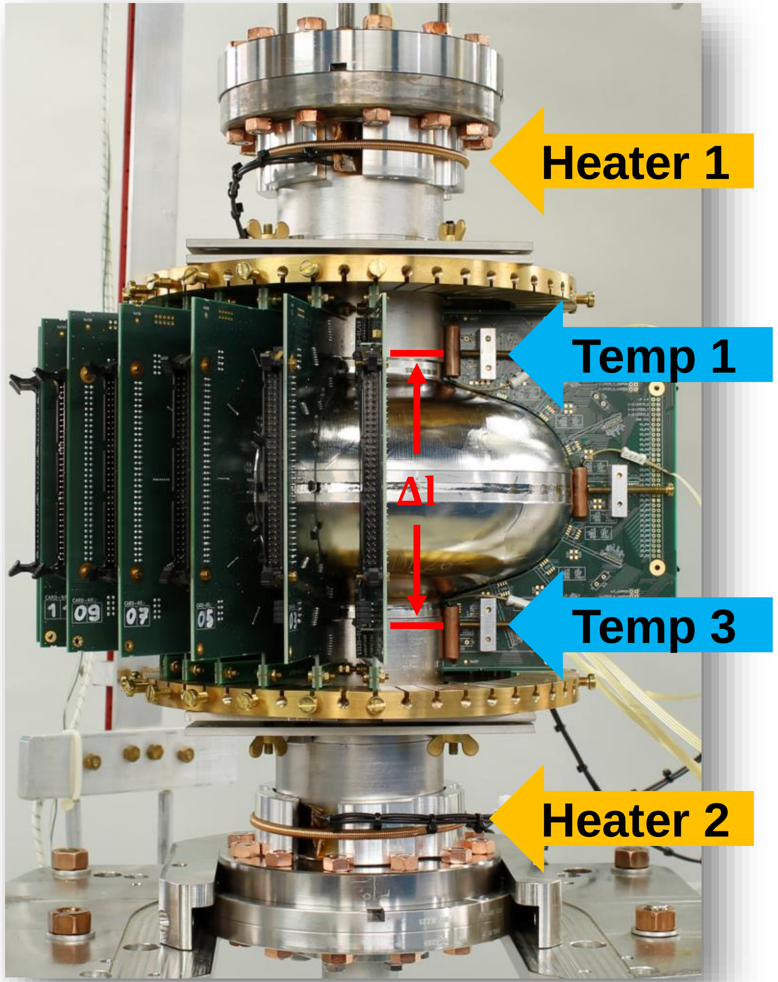

temperature gradient ∇T:

$$\nabla T = \frac{|Temp\,1 - Temp\,3|}{\Delta l = 225\ mm}$$

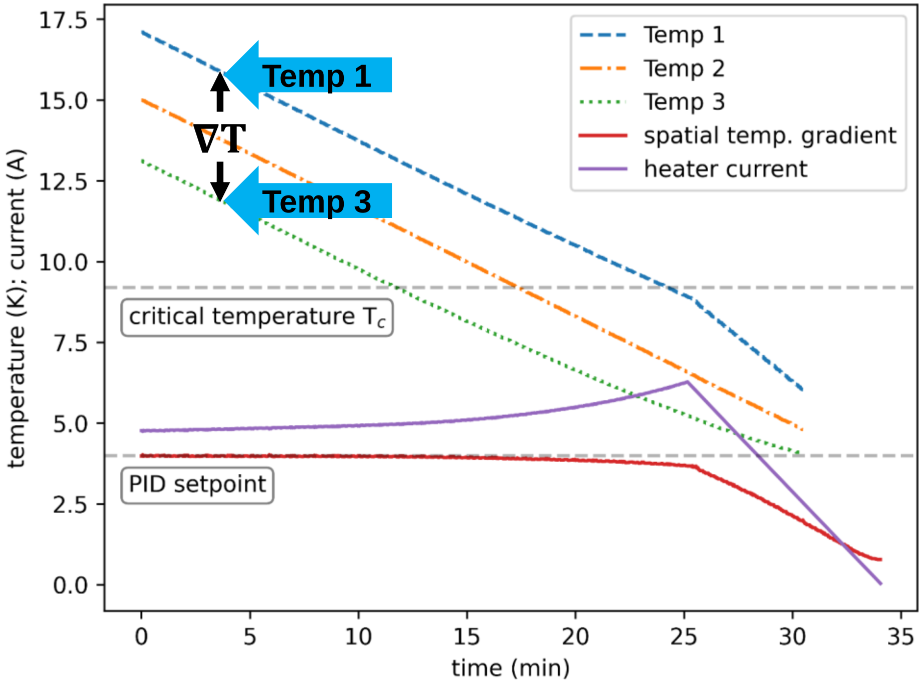

PID Controlled Spatial Temperature Gradient

➢ Suppress Stray Impact of a Changed Cool Down Velocity

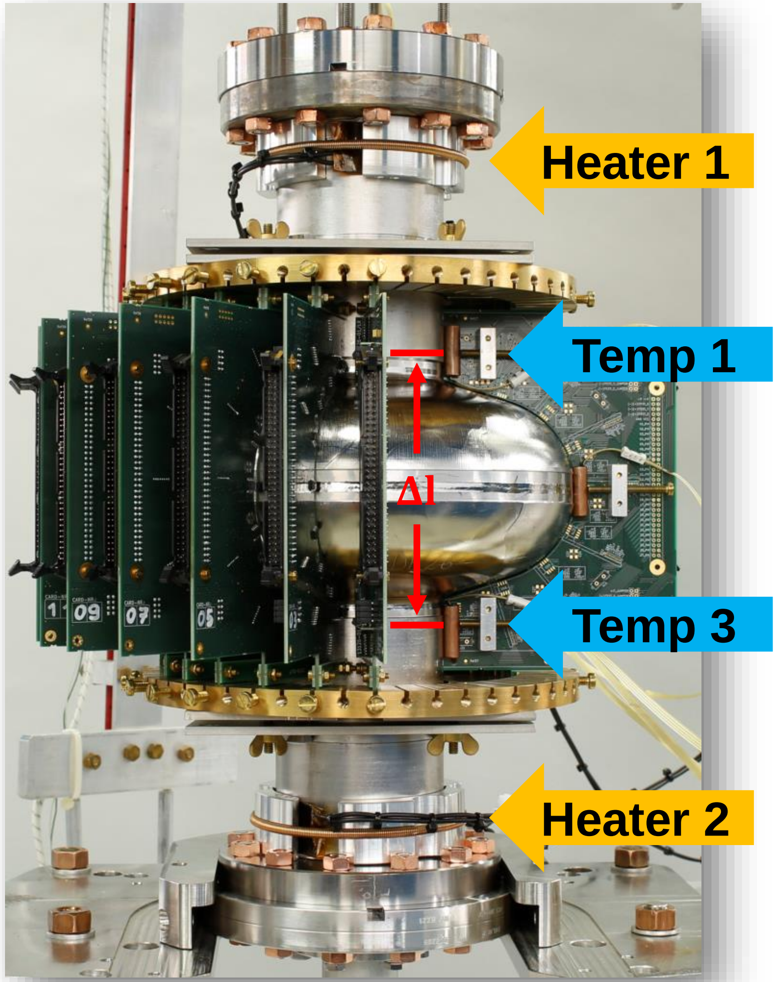

temperature gradient ∇T:

$$\nabla T = \frac{|Temp\,1 - Temp\,3|}{\Delta l = 225\ mm}$$

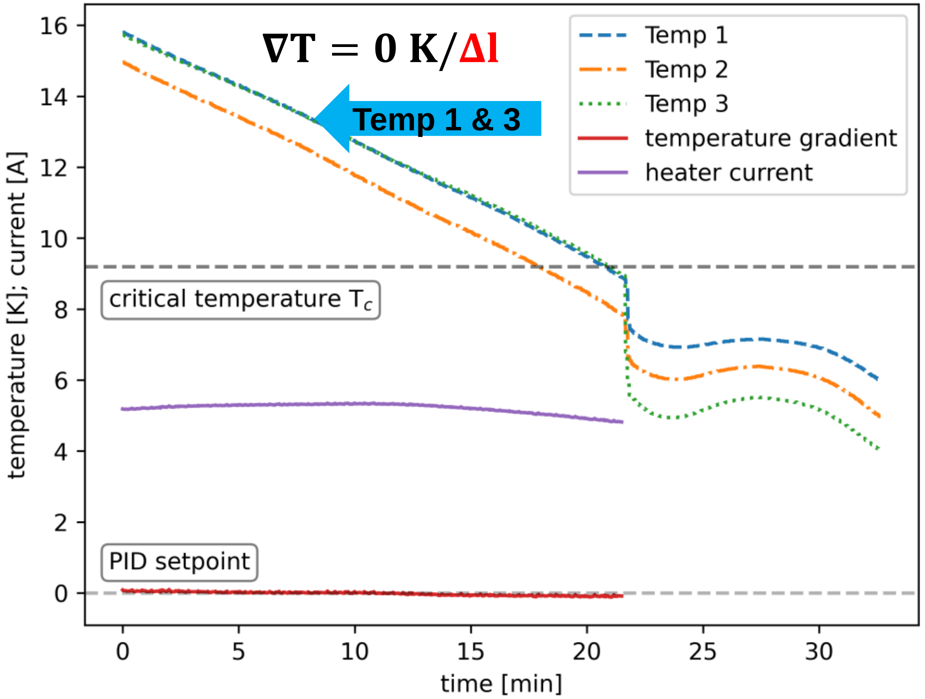

PID Controlled Spatial Temperature Gradient

➢ Suppress Stray Impact of a Changed Cool Down Velocity

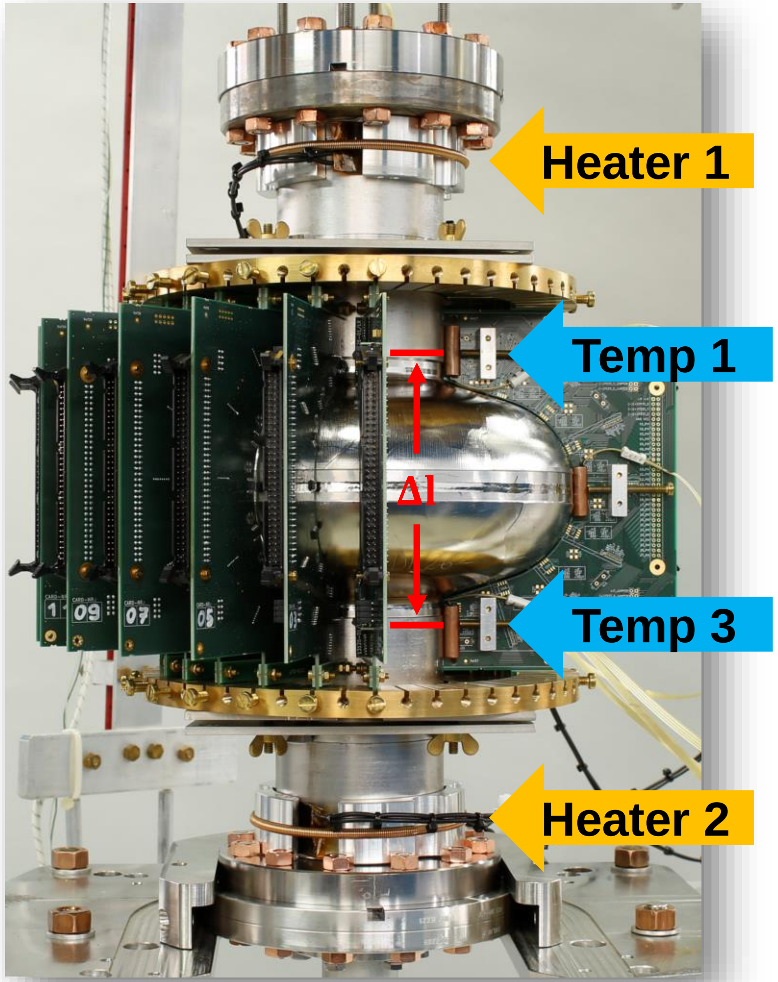

temperature gradient ∇T:

$$\nabla T = \frac{|Temp\ 1 - Temp\ 3|}{\Delta l = 225\ mm}$$

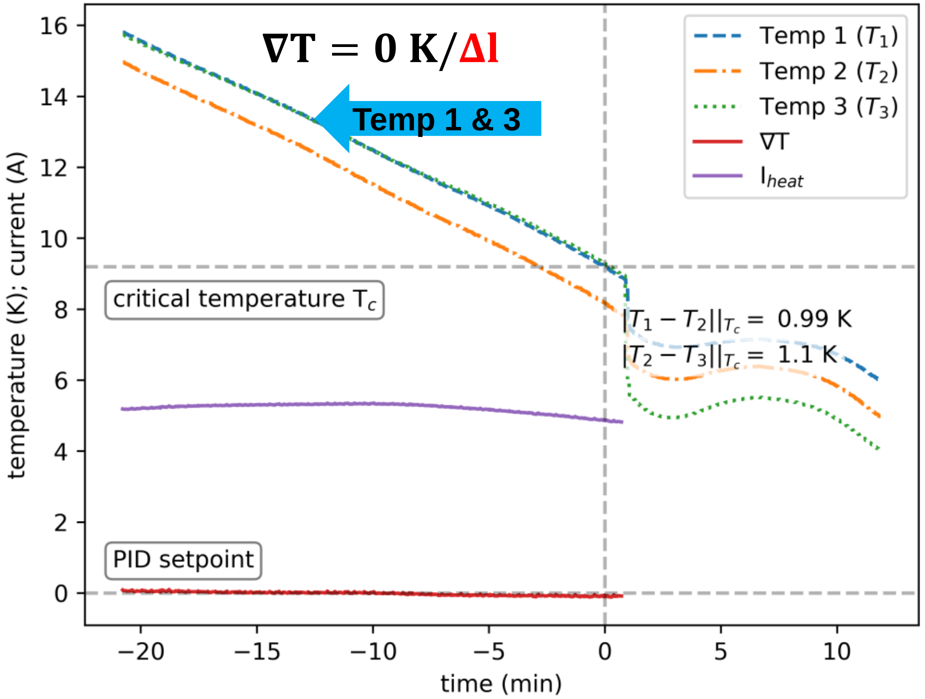

- ➢ residual difference between target **∇T** and real **∇T**
- ➢ $|T_1 - T_2|_{Tc}$ and $|T_2 - T_3|_{Tc}$ used for cool down comprehensive comparisons

Compute Ideal Flux Expulsion Ratio B_{sc} / B_{nc}

➢ Obtain Fraction of Magnetic Flux Trapped

common approach: simulation of cavity in ideal Meissner state

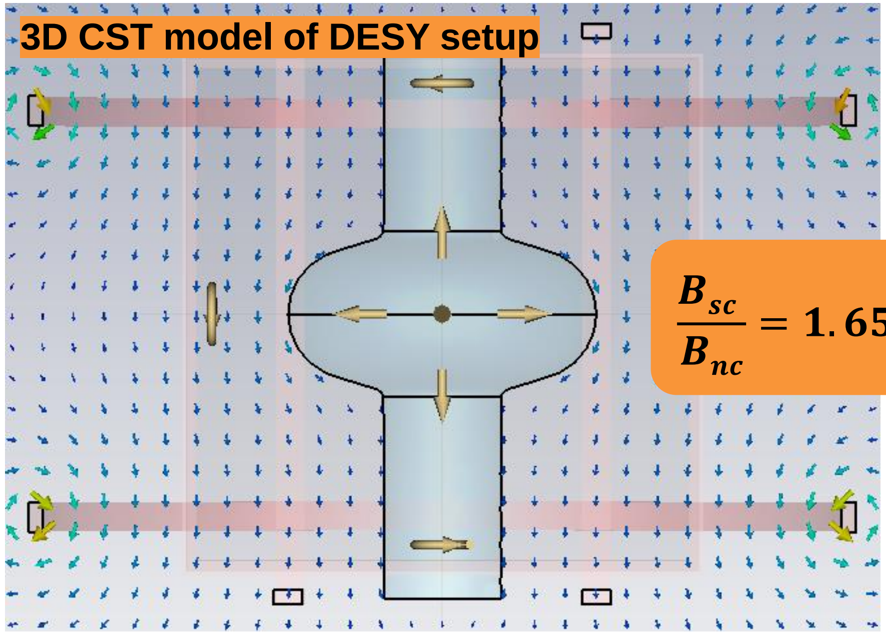

$$\frac{B_{sc}}{B_{nc}} = 1.65$$

Akira Miyazaki:
high deviation between simulation and experimental data observed → likelely caused by a neglected partial flux shielding by cavity flanges

alternative experimental approach (Kensei Unemori):

1. cool down cavity (Meissner state)
2. apply magnetic field by Helmholtz coil
3. measure B_{sc} (ideal Meissner state)
4. warm up cavity (normal conducting state)
5. measure B_{nc}

axially symmetrical problem:

- ➢ 2D magnetostatic solver Pandira (Poisson Superfish)
- ➢ high resolution mesh

Compute Ideal Flux Expulsion Ratio B_{sc} / B_{nc}

Model 1: Cavity in Normal Conducting (nc) State → obtain B_{nc}

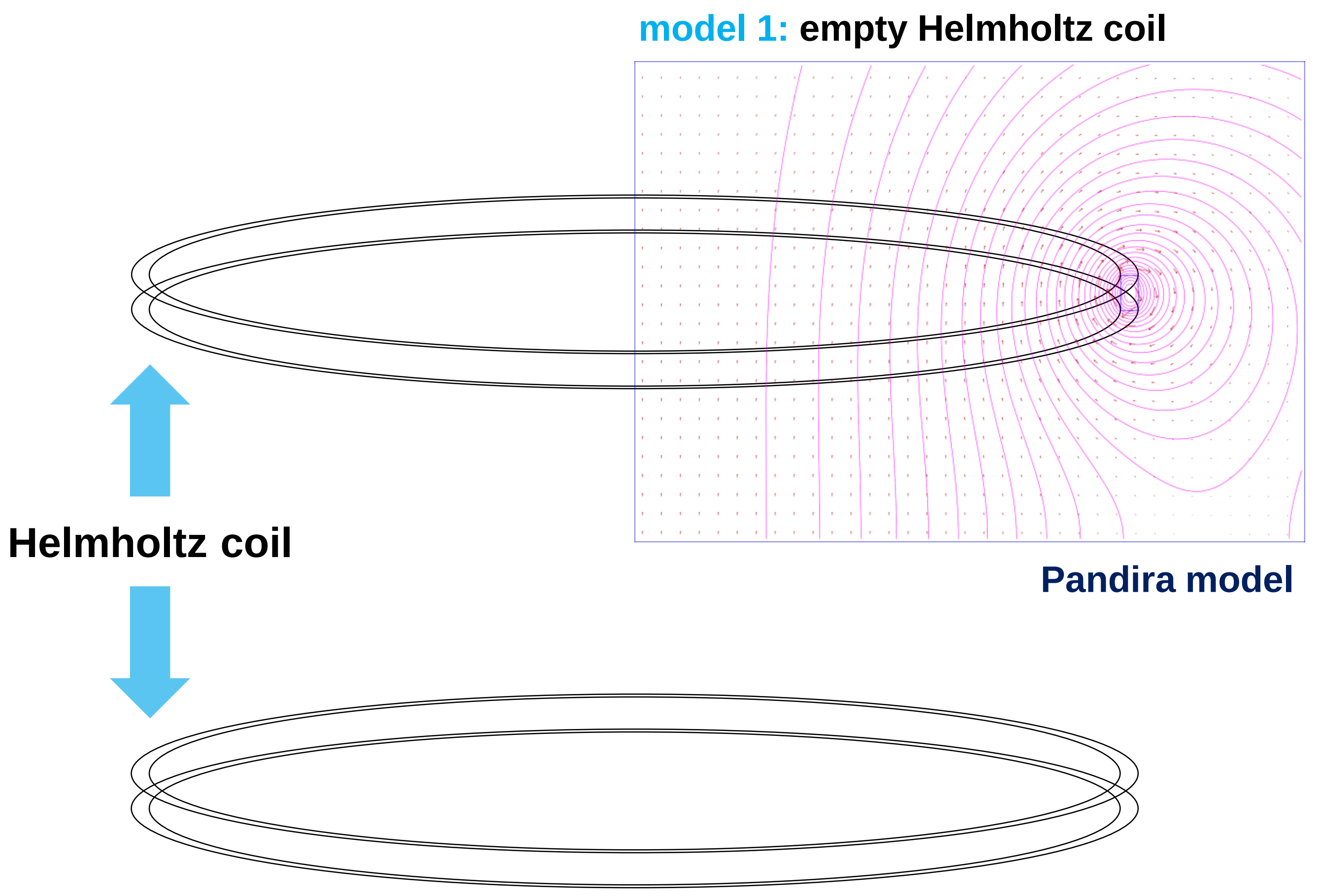

Compute Ideal Flux Expulsion Ratio B_{sc} / B_{nc}

Model 2: Cavity (simplified) in Superconducting (sc1) State → obtain B_{sc1}

model 1: empty Helmholtz coil

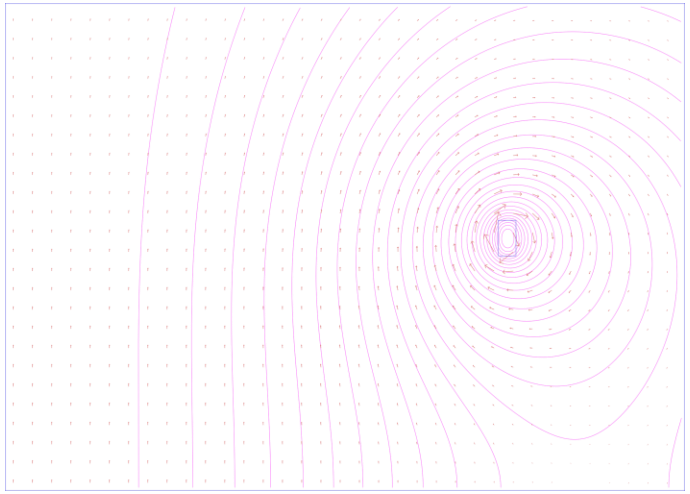

model 2: single cell cavity (simplified)

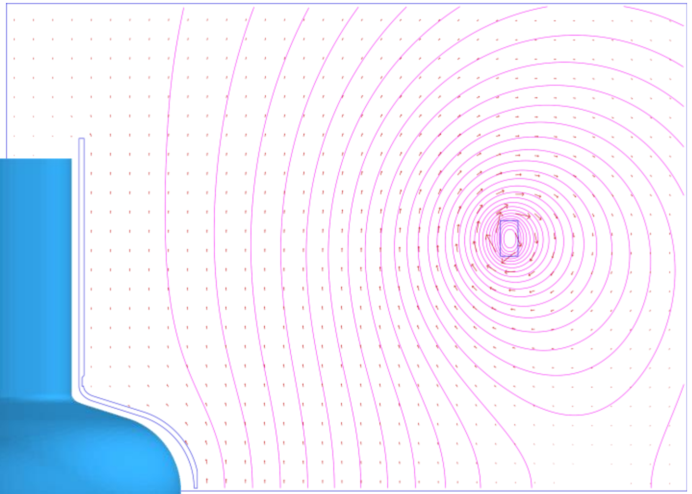

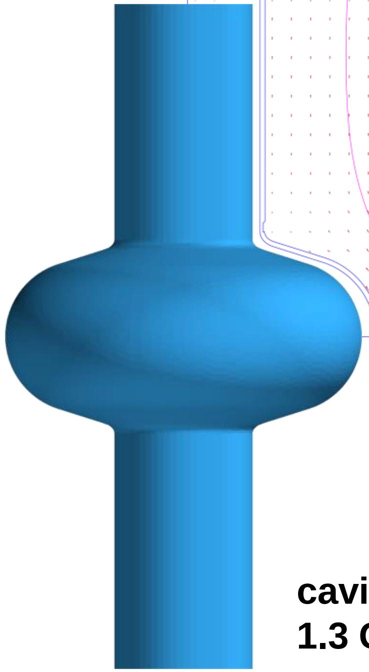

cavity shape:
1.3 GHz TESLA Type

Compute Ideal Flux Expulsion Ratio B_{sc} / B_{nc}

Model 3: Cavity (detailed) in Superconducting (sc2) State → obtain B_{sc2}

model 1: empty Helmholtz coil

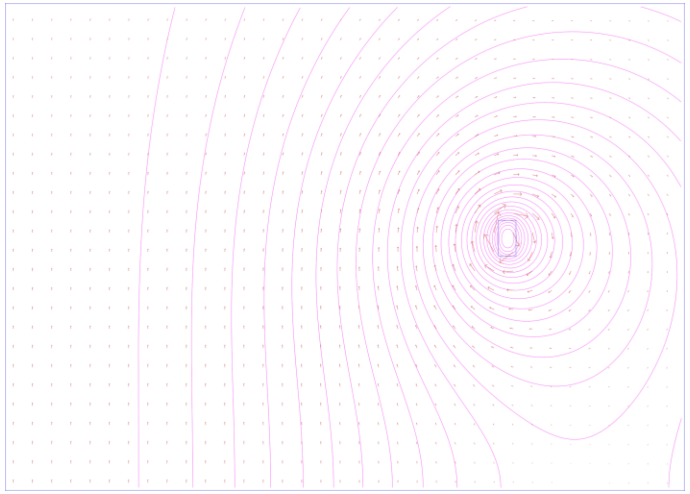

model 2: single cell cavity (simplified)

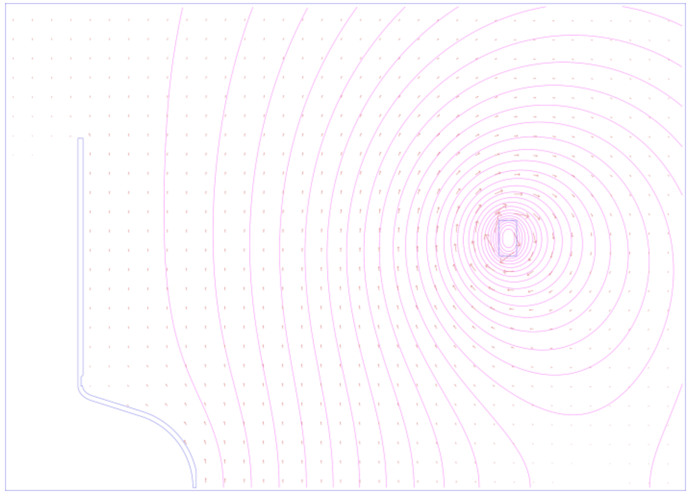

model 3: single cell cavity (detailed)

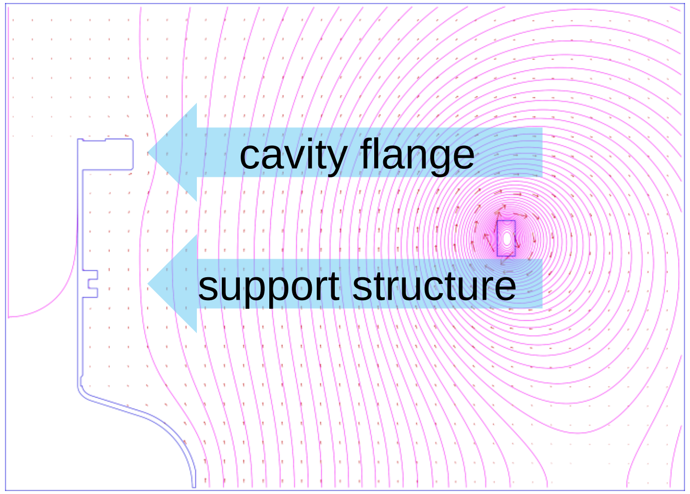

Compute Ideal Flux Expulsion Ratio B_{sc} / B_{nc}

Model 3: Cavity (detailed) in Superconducting (sc2) State → obtain B_{sc2}

model 1: empty Helmholtz coil

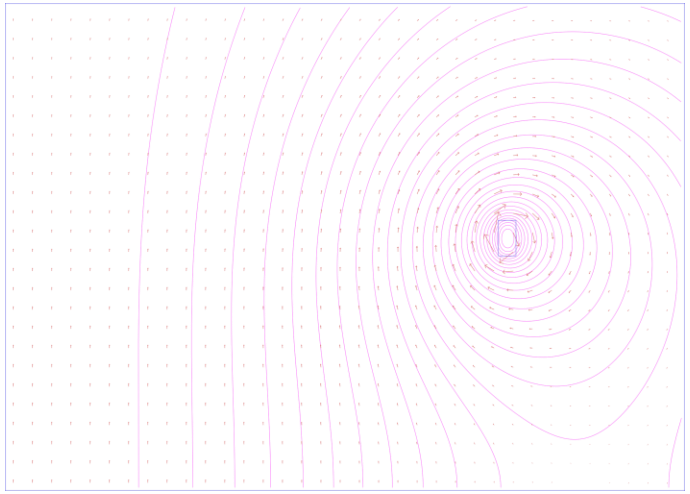

model 2: single cell cavity (simplified)

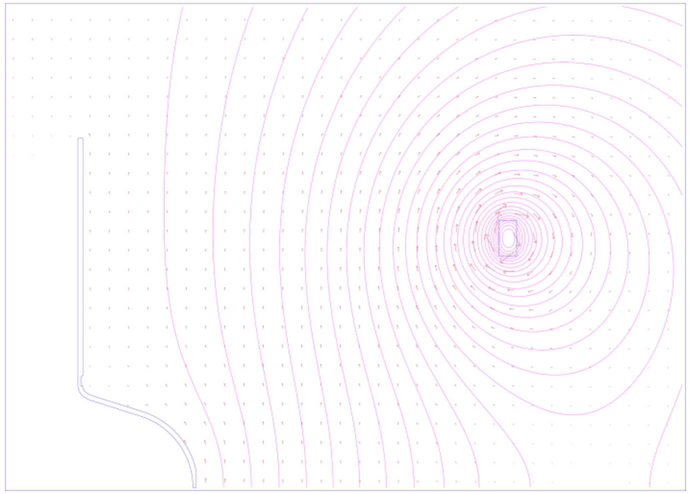

model 3: single cell cavity (detailed)

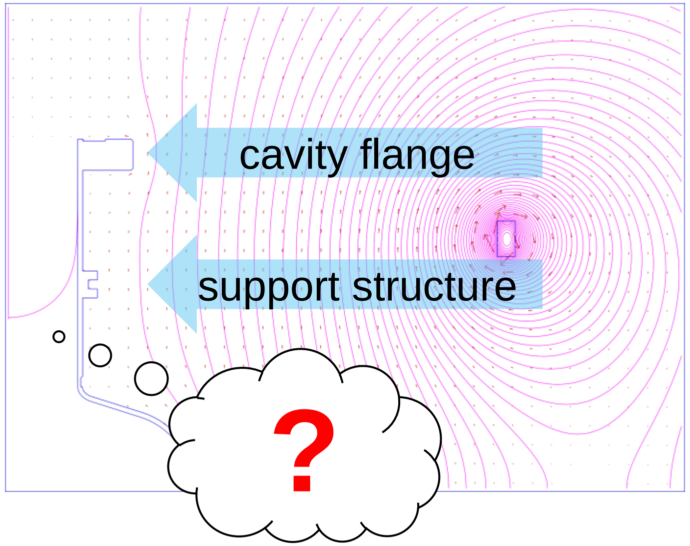

Compute Ideal Flux Expulsion Ratio B_{sc} / B_{nc}

- Extract B_{nc}, B_{sc1} and B_{sc2} from Models for first 30 mm from Equator Surface

model 1: empty Helmholtz coil

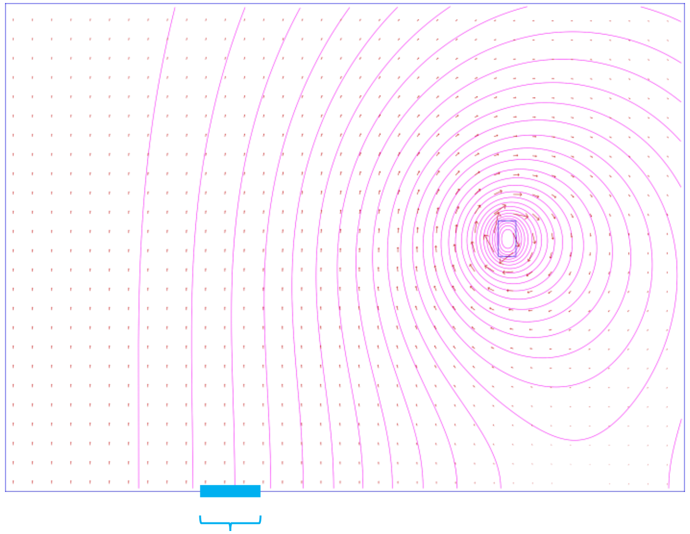

B_{nc}

model 2: single cell cavity (simplified)

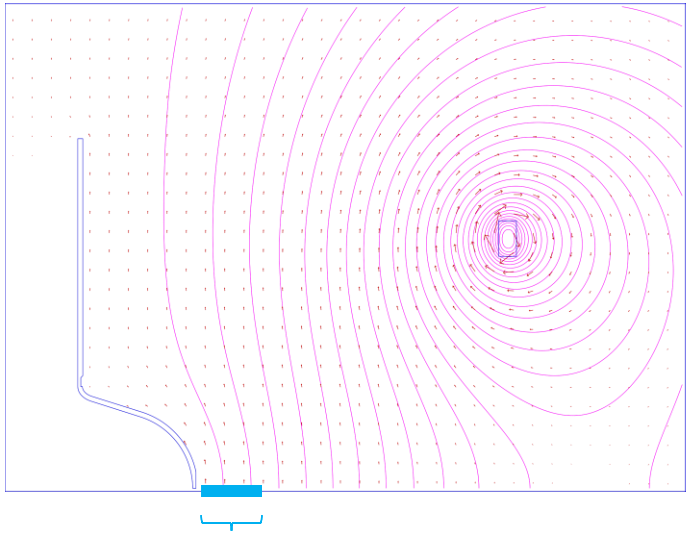

B_{sc1}

model 3: single cell cavity (detailed)

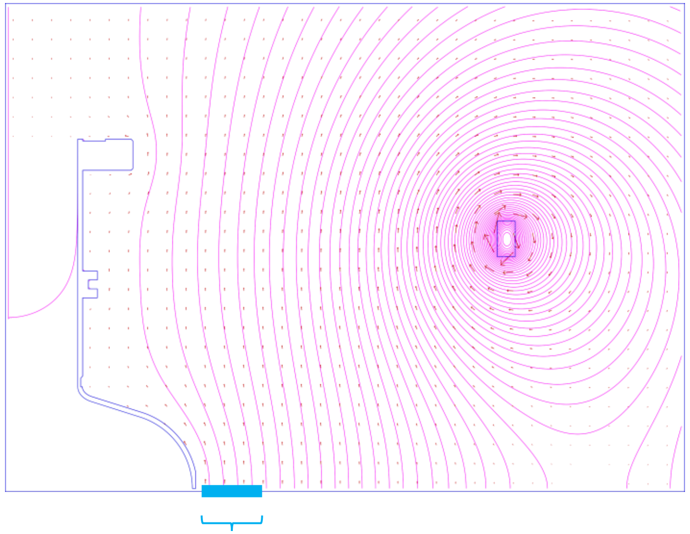

B_{sc2}

Compute Ideal Flux Expulsion Ratio B_{sc} / B_{nc}

➢ Extract B_{nc}, B_{sc1} and B_{sc2} from Models for first 30 mm from Equator Surface

model 1: **empty Helmholtz coil**

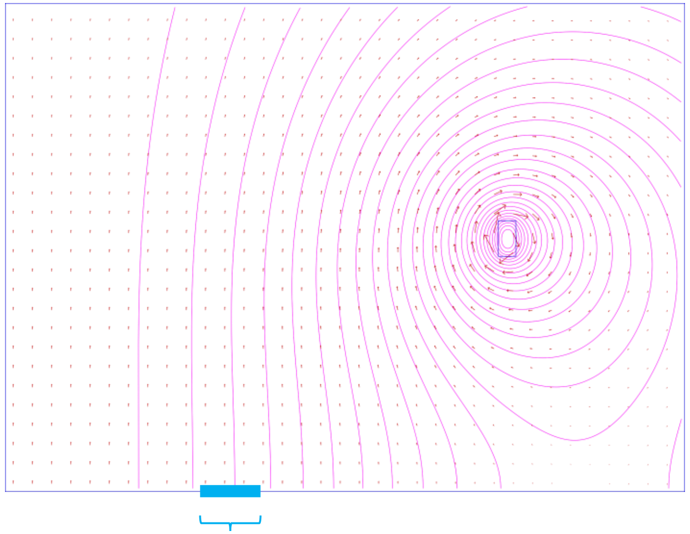

B_{nc}

model 2: **single cell cavity (simplified)**

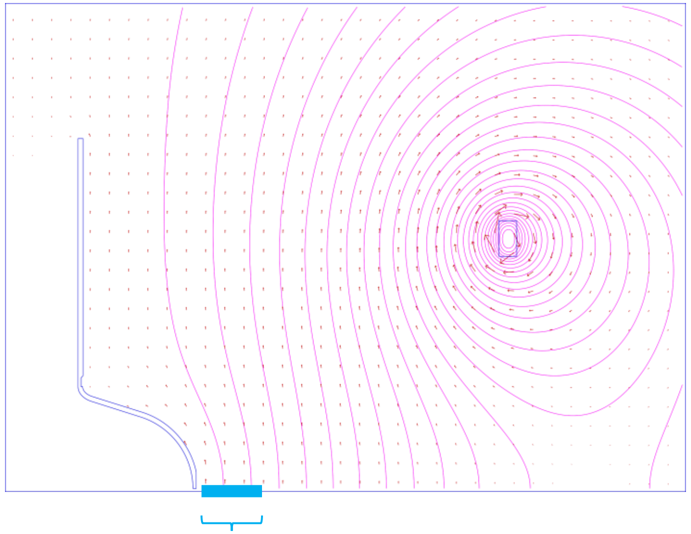

B_{sc1}

$$\frac{B_{sc1}}{B_{nc}}$$

model 3: **single cell cavity (detailed)**

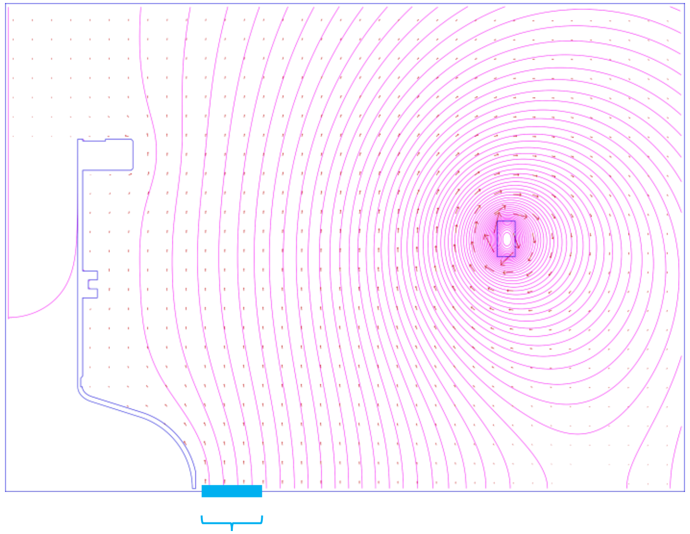

B_{sc2}

$$\frac{B_{sc2}}{B_{nc}}$$

Compute Ideal Flux Expulsion Ratio B_{sc} / B_{nc}

➢ **Visible Impact of Flux Shielding Effect by NbTi Flanges**

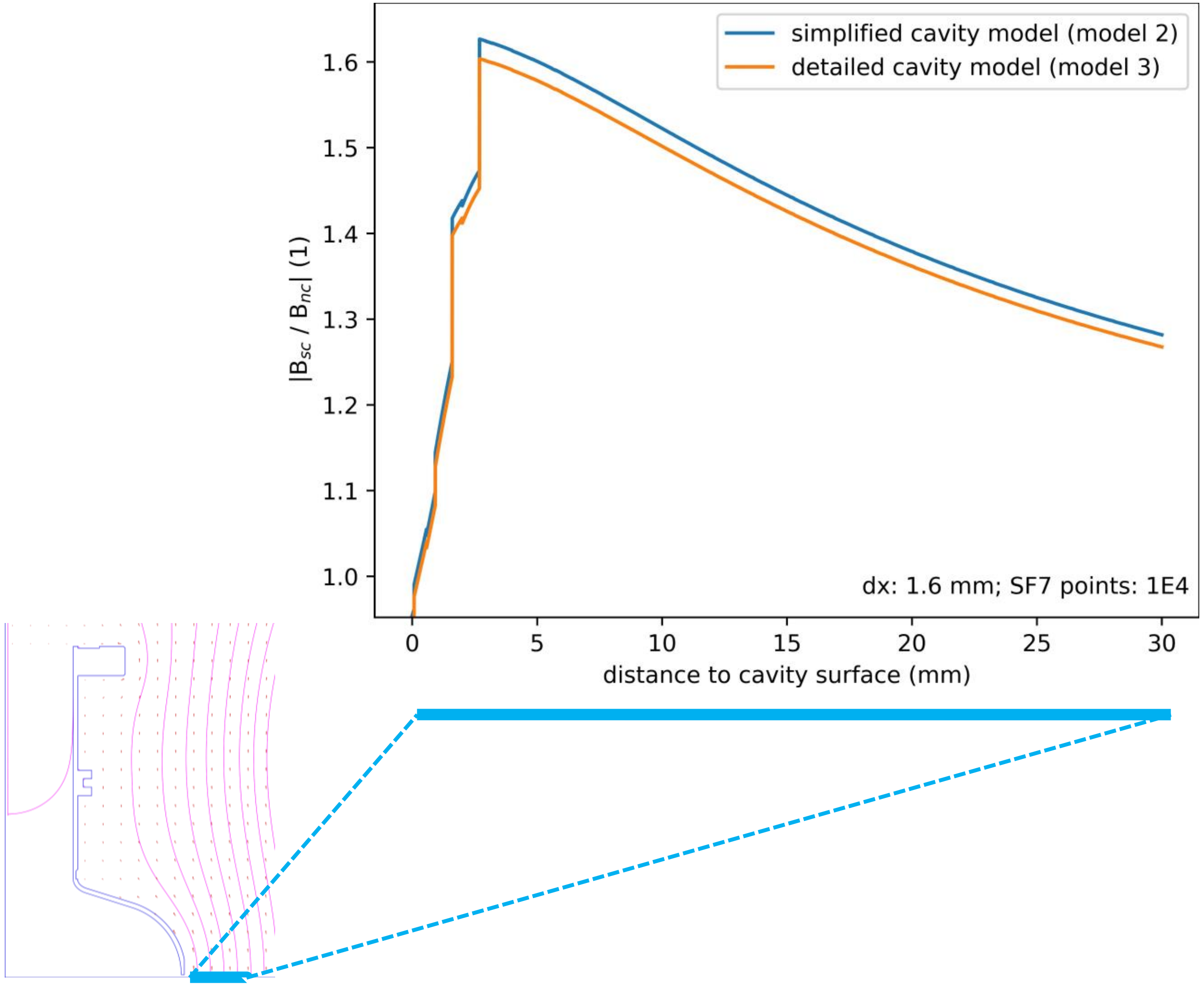

Compute Ideal Flux Expulsion Ratio B_{sc} / B_{nc}

➢ High Resolution Mesh Crucial for Accurate Simulations

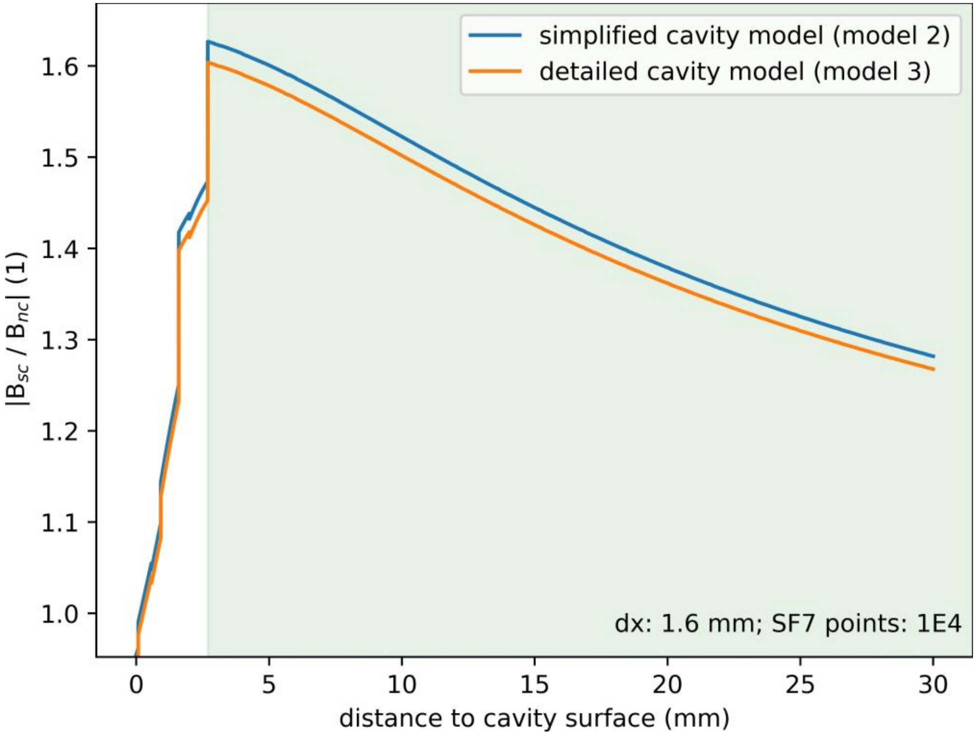

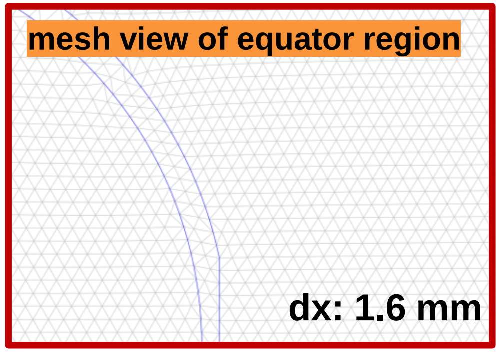

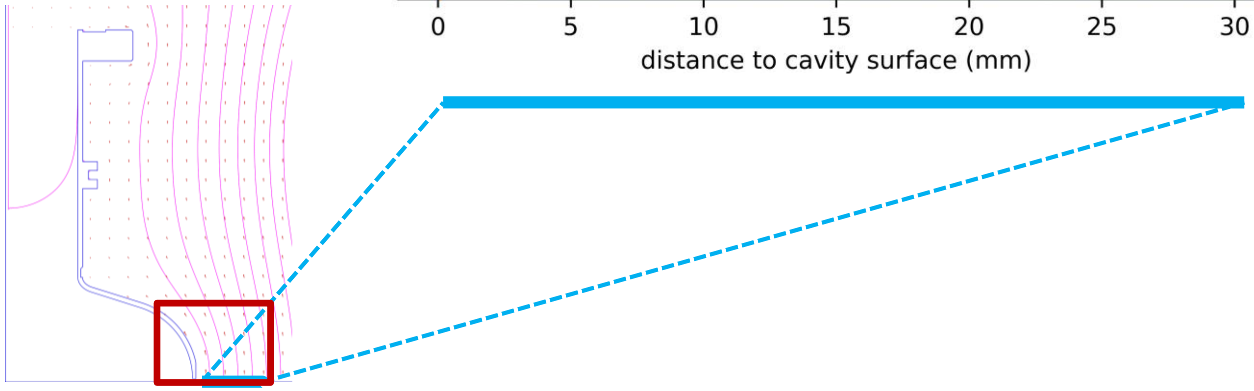

Compute Ideal Flux Expulsion Ratio B_{sc} / B_{nc}

➢ **High Resolution Mesh Crucial for Accurate Simulations**

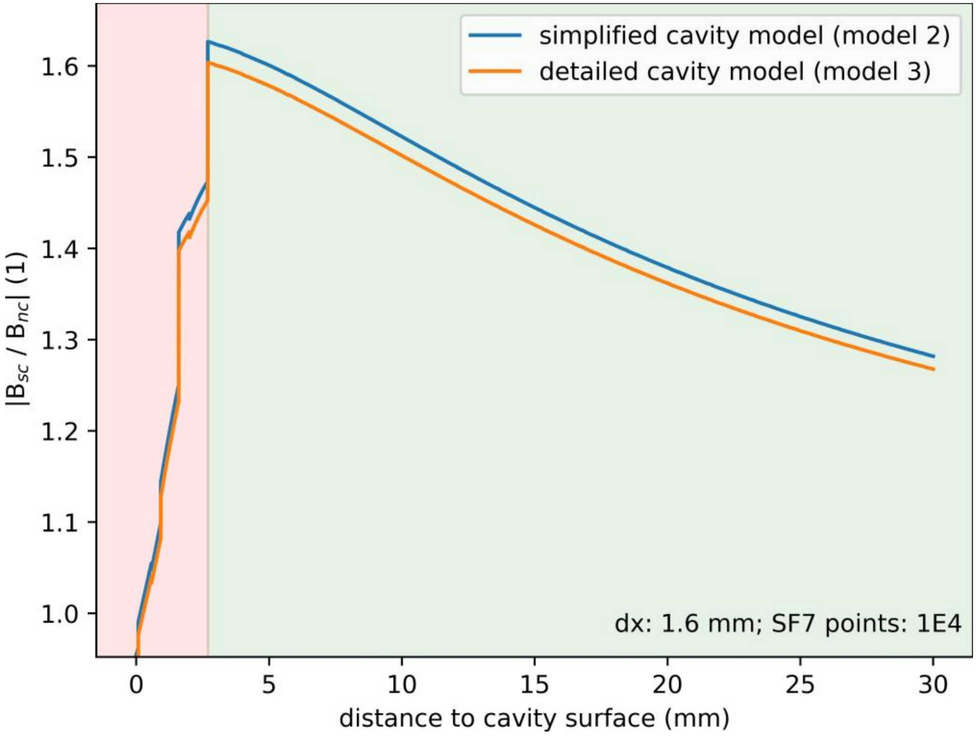

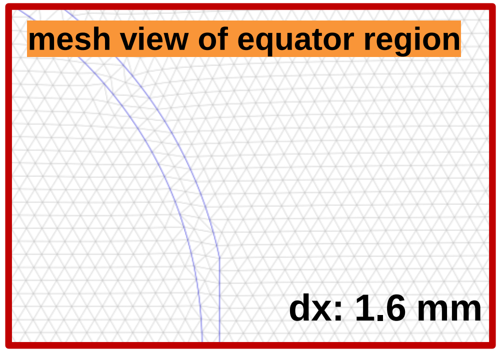

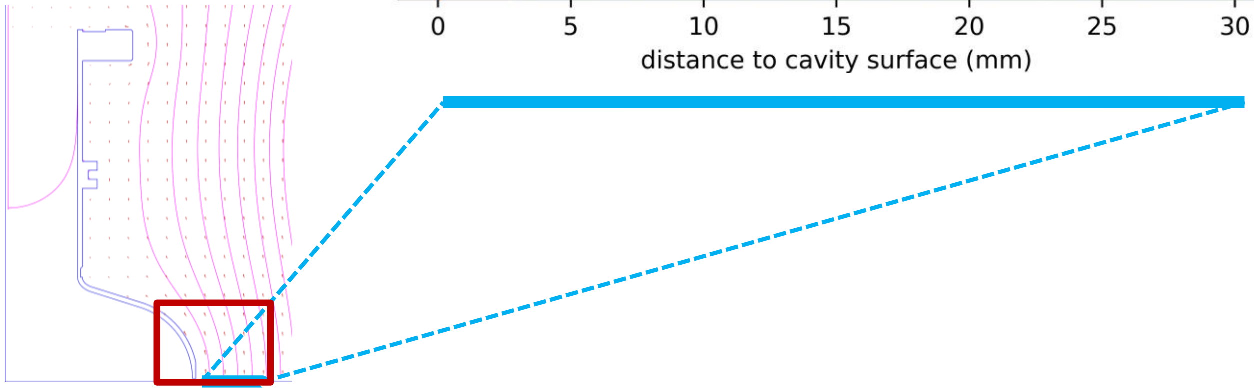

Compute Ideal Flux Expulsion Ratio B_{sc} / B_{nc}

➢ **High Resolution Mesh Crucial for Accurate Simulations**

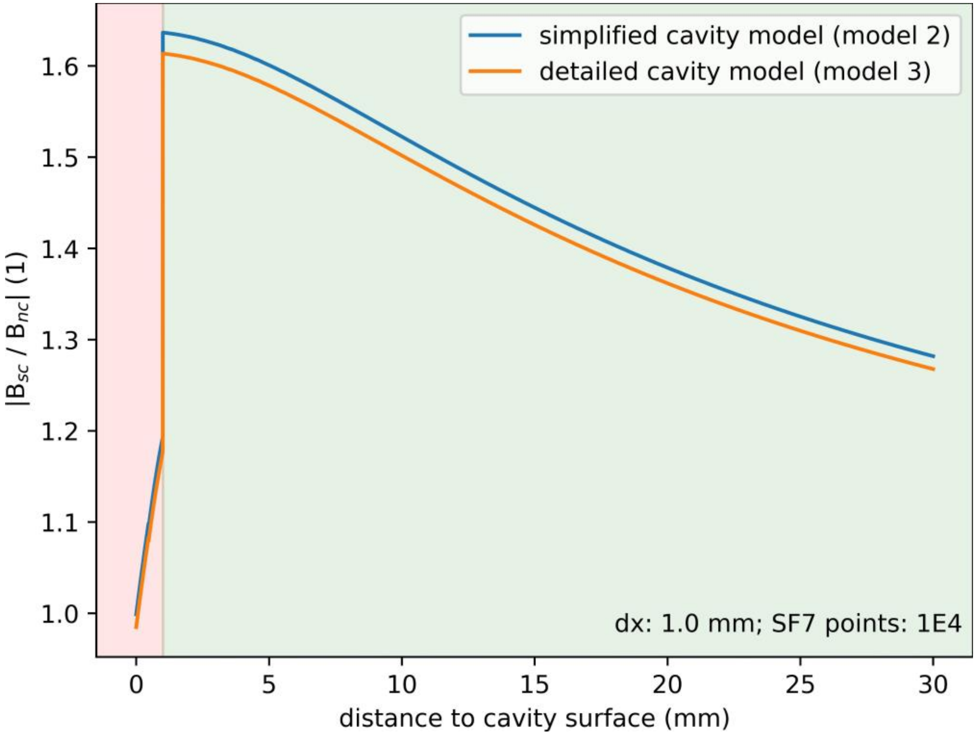

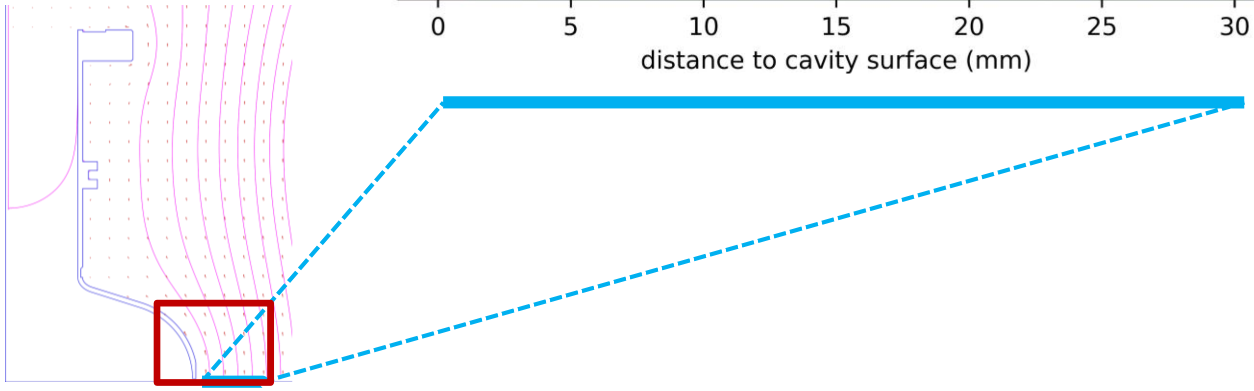

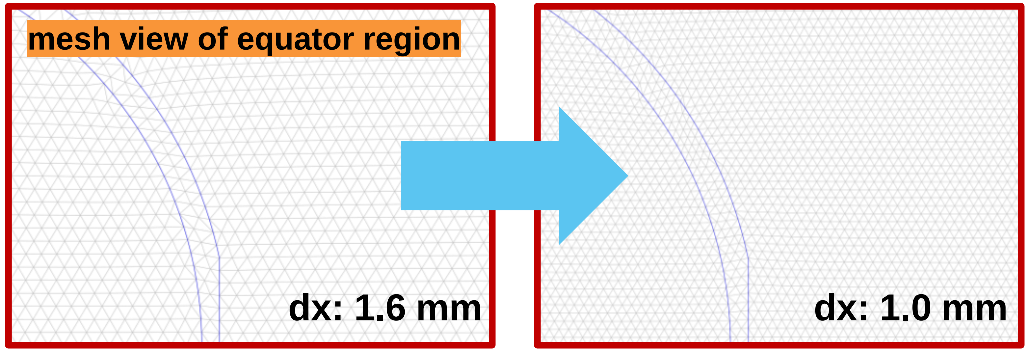

Compute Ideal Flux Expulsion Ratio B_{sc} / B_{nc}

➢ High Resolution Mesh Crucial for Accurate Simulations

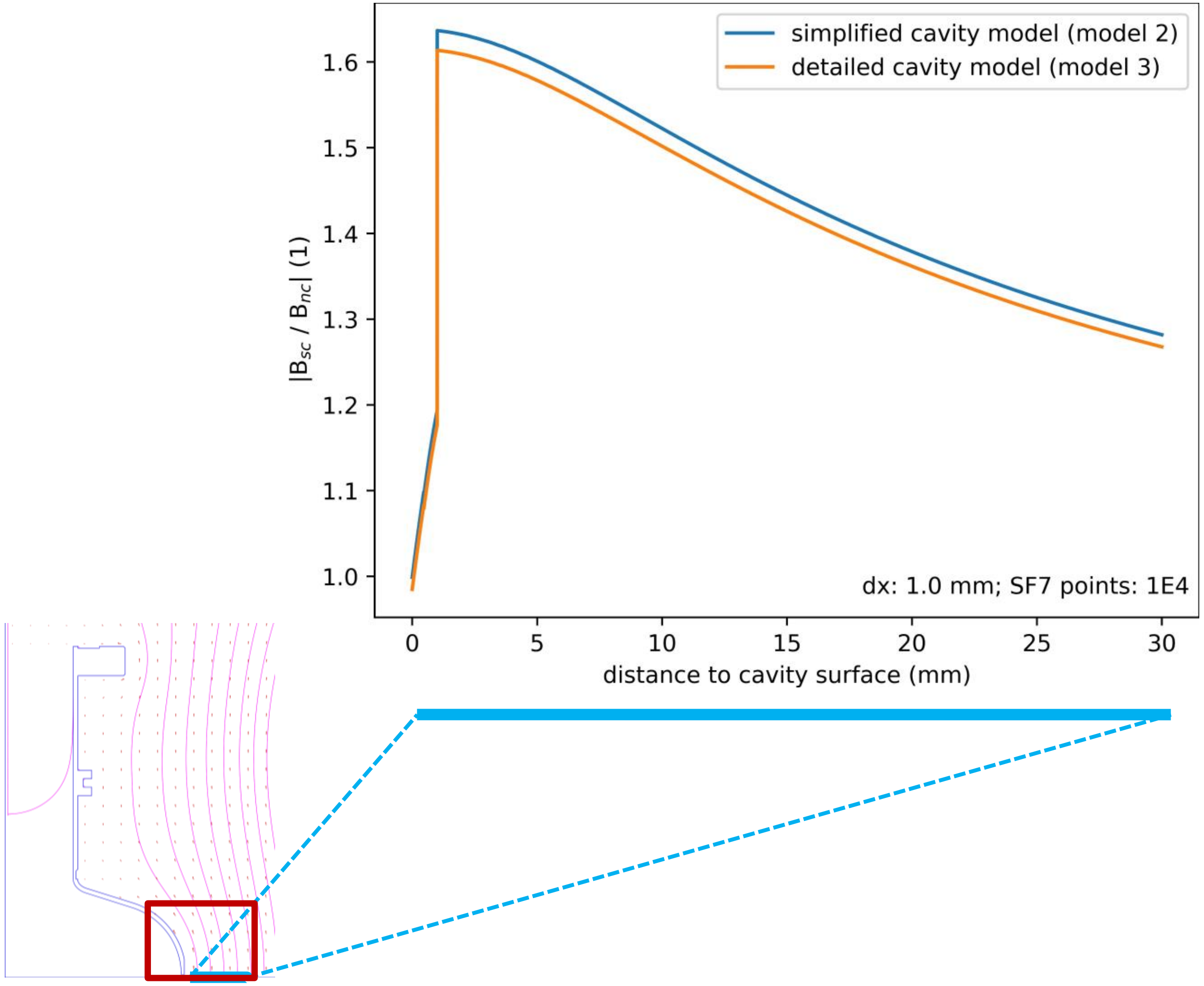

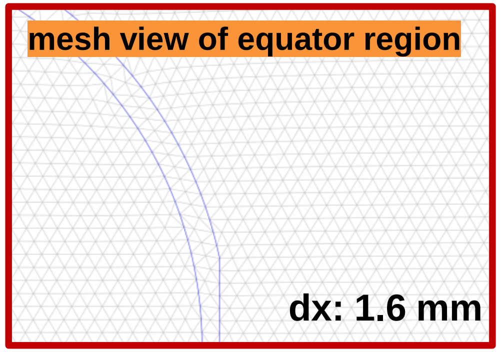

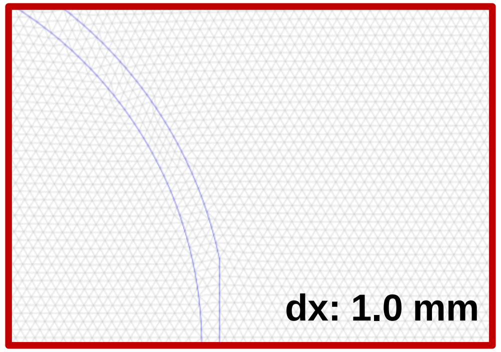

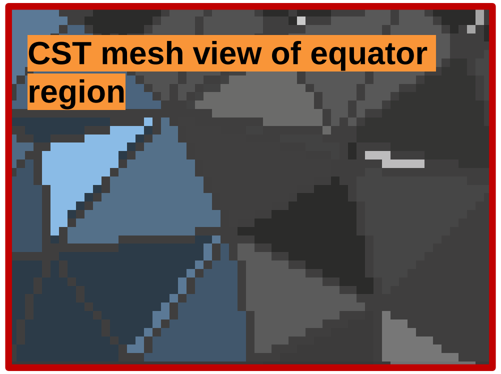

- ➢ 3D CST mesh was chosen to coarse for accurate simulations
- ➢ cross-check simulation results by experimental approach

Compute Ideal Flux Expulsion Ratio B_{sc} / B_{nc}

➢ High Resolution Mesh Crucial for Accurate Simulations

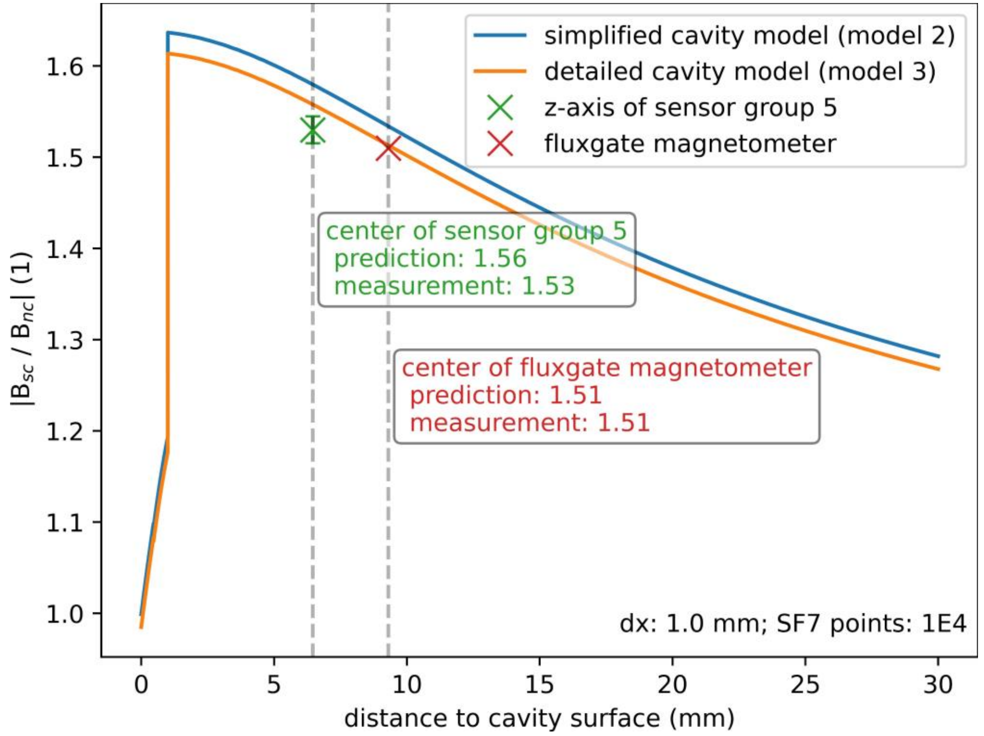

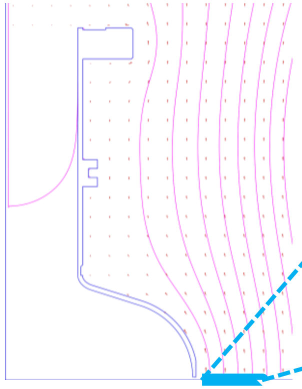

experimental approach (K. Unemori):

1. cool down cavity (Meissner state)
2. apply magnetic field by Helmholtz coil
3. measure B_{sc} (ideal Meissner state)
4. warm up cavity (normal conducting state)
5. measure B_{nc}

fluxgate mag. (Bartington Mag F Probe)

- center point distance to surface: 9.3 mm
- simulation & measurement identical: B_{sc} / B_{nc} = 1.51

z axis of equator sensor group (group 5)

- mean value of all 23 boards
- error bar: 2σ
- simulation: B_{sc} / B_{nc} = 1.56
- measurement: B_{sc} / B_{nc} = 1.53

Compute Ideal Flux Expulsion Ratio B_{sc} / B_{nc}

➢ High Resolution Mesh Crucial for Accurate Simulations

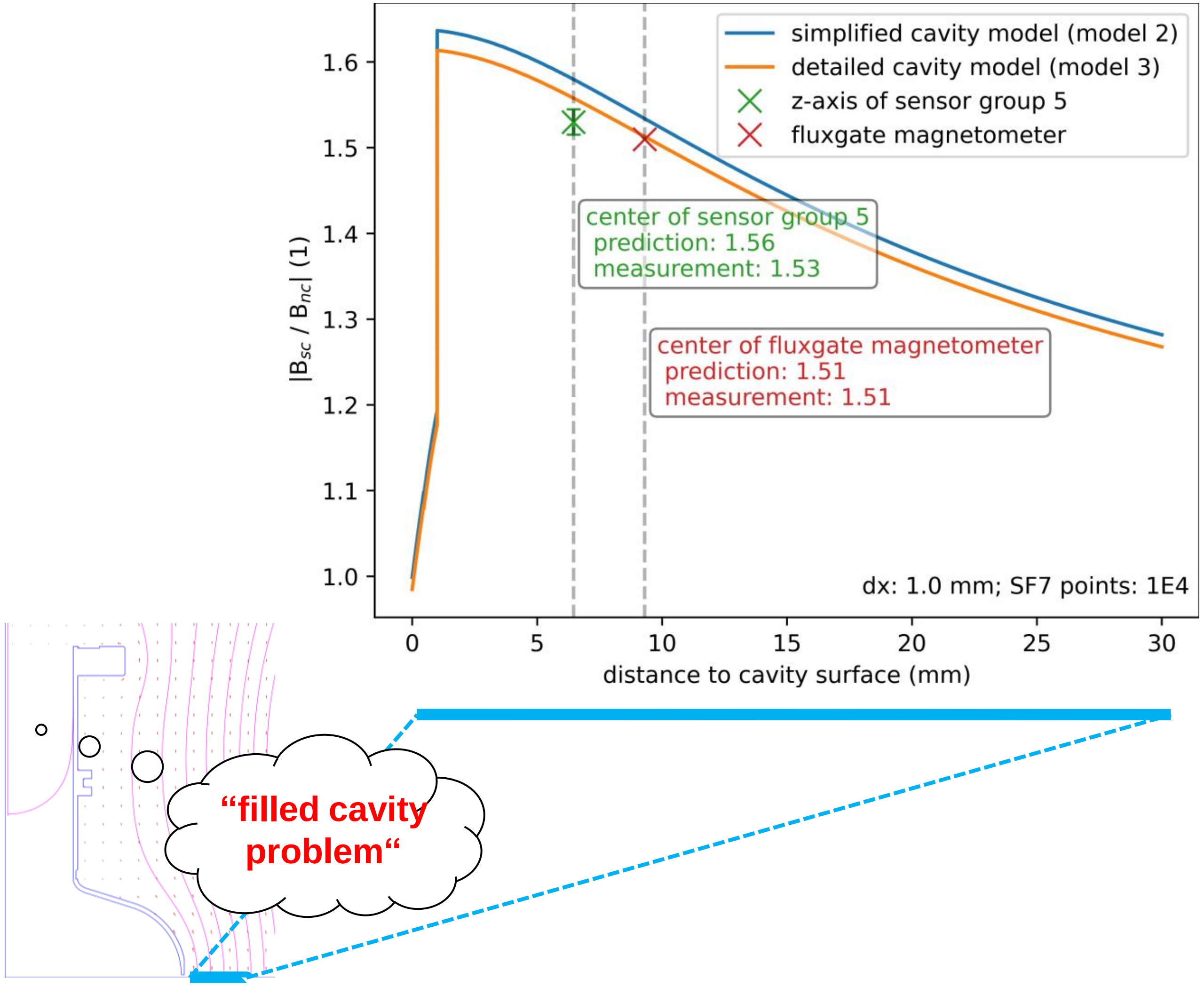

experimental approach (K. Unemori):

1. cool down cavity (Meissner state)
2. apply magnetic field by Helmholtz coil
3. measure B_{sc} (ideal Meissner state)
4. warm up cavity (normal conducting state)
5. measure B_{nc}

fluxgate mag. (Bartington Mag F Probe)

- center point distance to surface: 9.3 mm
- simulation & measurement identical: B_{sc} / B_{nc} = 1.51

z axis of equator sensor group (group 5)

- mean value of all 23 boards
- error bar: 2σ
- simulation: B_{sc} / B_{nc} = 1.56
- measurement: B_{sc} / B_{nc} = 1.53

Polar Plot of Equator Flux Expulsion Ratios

➢ Measured Expulsion Ratios as a Function of Card Identifier

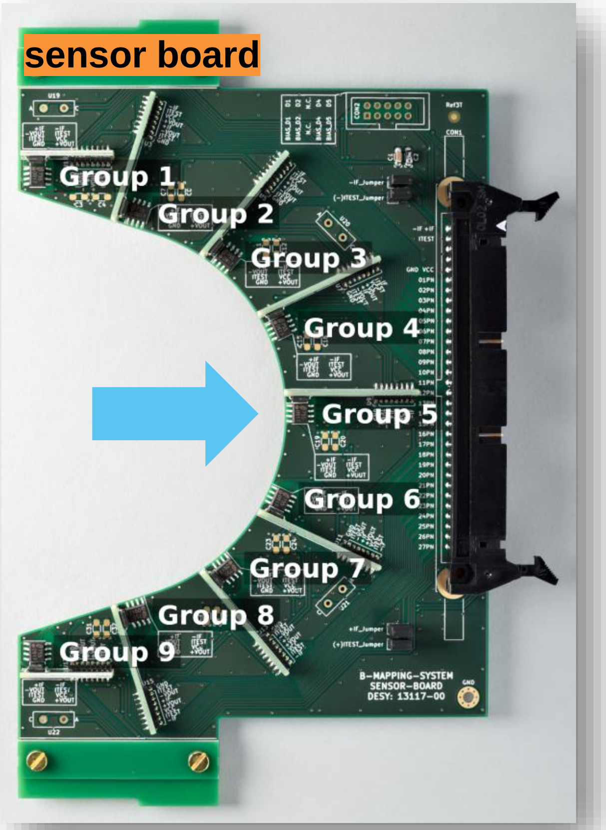

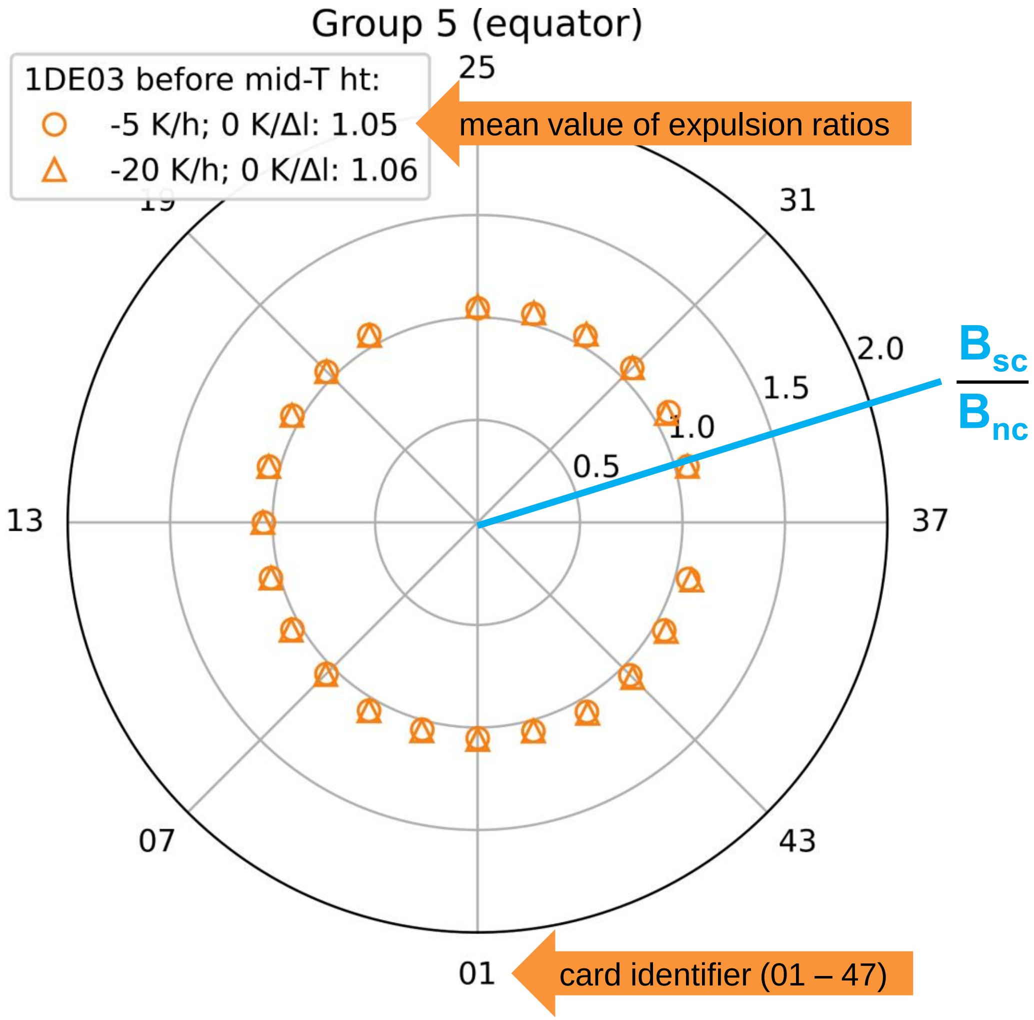

Results: Impact of Cooldown Velocity on B_{sc} / B_{nc}

➢ **(Likely) No Impact of Cool Down Velocity on Flux Expulsion Behavior**

1DE03 fine-grain material
before mid-T heat treatment

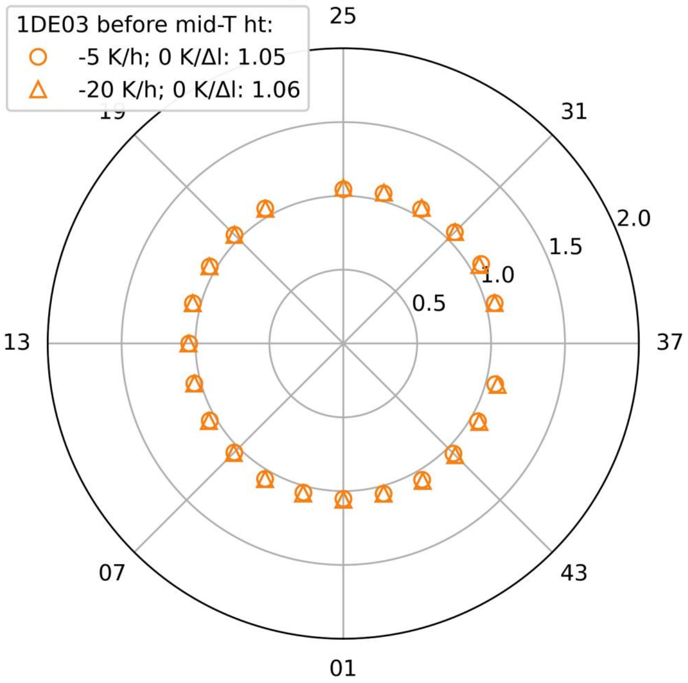

-5 K/h; 0 K/ΔI: 90 % fraction of B (10 µT) trapped

-20 K/h; 0 K/ΔI: 89 % fraction of B (10 µT) trapped

Results: Impact of Cooldown Velocity on B_{sc} / B_{nc}

➢ **(Likely) No Impact of Cool Down Velocity on Flux Expulsion Behavior**

1DE03 fine-grain material
before mid-T heat treatment

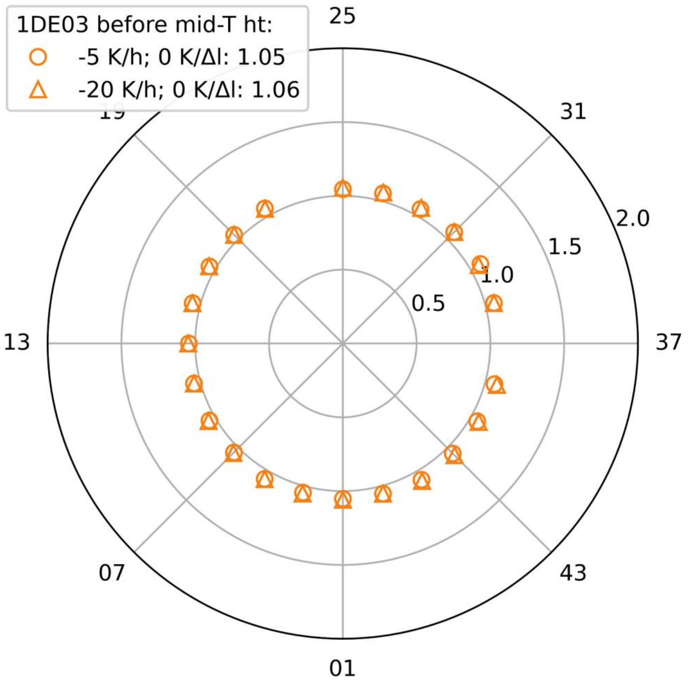

1DE09 fine-grain material
after mid-T heat treatment

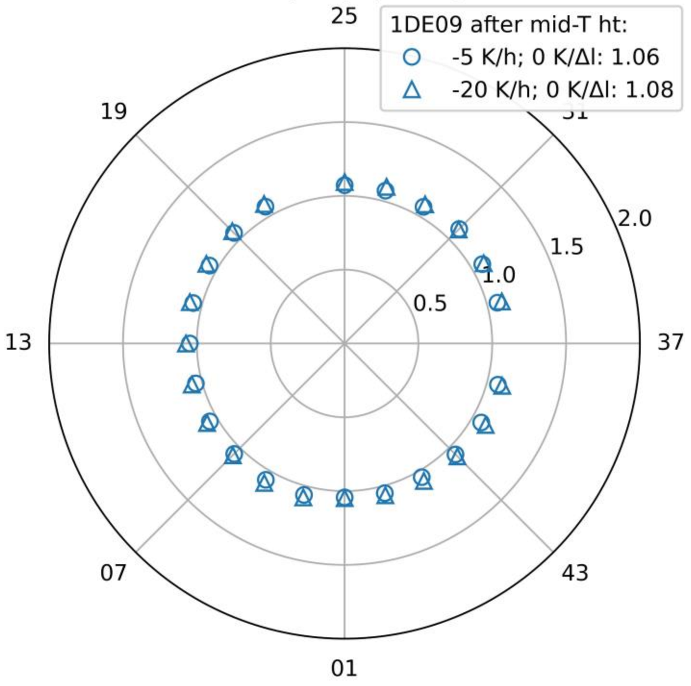

-5 K/h; 0 K/ΔI:	90 %	- %	**-5 K/h; 0 K/ΔI:**	- %	88 %
-20 K/h; 0 K/ΔI:	89 %	- %	**-20 K/h; 0 K/ΔI:**	- %	84 %

Results: Impact of Cooldown Velocity on B_{sc} / B_{nc}

➢ **(Likely) No Impact of Cool Down Velocity on Flux Expulsion Behavior**

1DE03 fine-grain material
before mid-T heat treatment

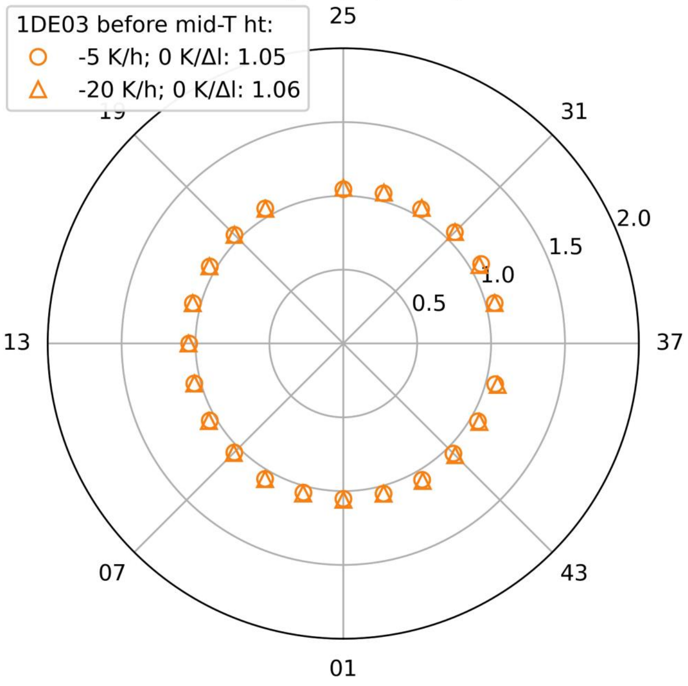

1DE09 fine-grain material
after mid-T heat treatment

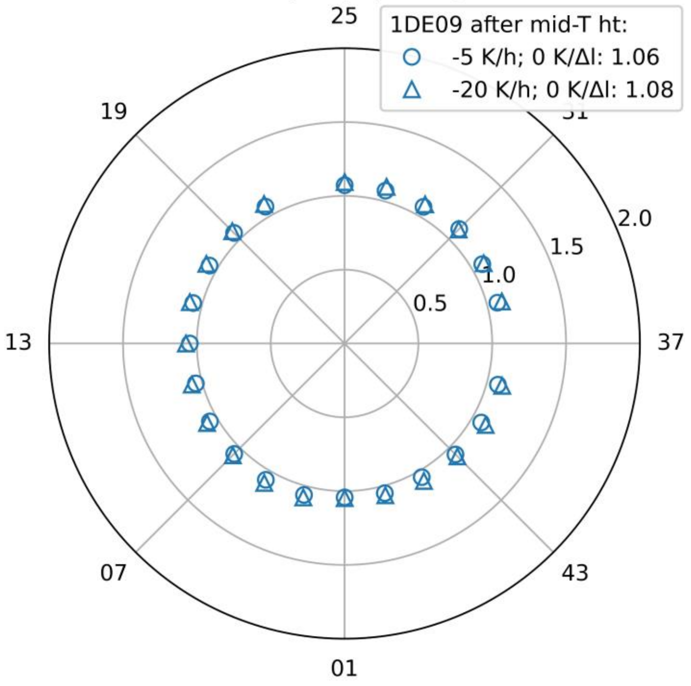

1DE26 large-grain material
before mid-T heat treatment

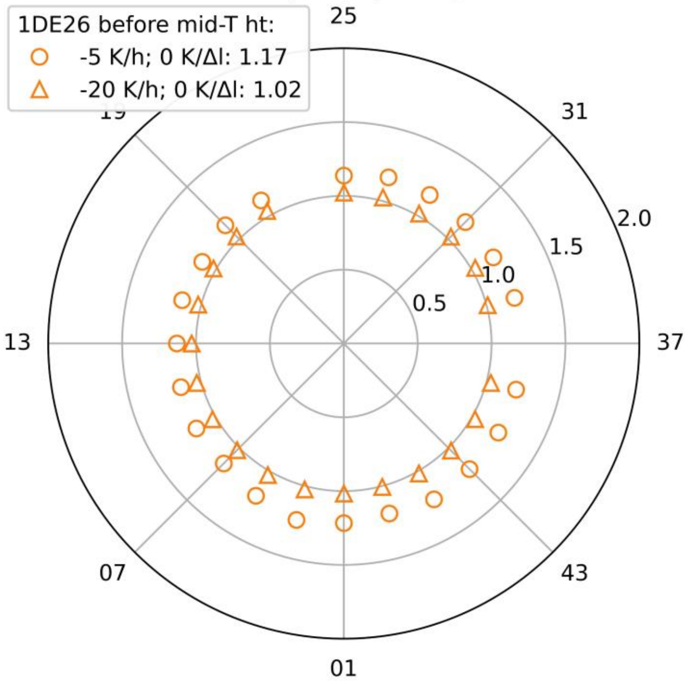

-5 K/h; 0 K/ΔI:	90 %	- %
-20 K/h; 0 K/ΔI:	89 %	- %

-5 K/h; 0 K/ΔI:	- %	88 %
-20 K/h; 0 K/ΔI:	- %	84 %

-5 K/h; 0 K/ΔI:	68 %
-20 K/h; 0 K/ΔI:	(96 %)

likely caused by deviant heater shutdown procedure

Results: Impact of Heater Shutdown Procedure on B_{sc} / B_{nc}

➢ Contradictory to Flux Expulsion Results: Real ∇T Decreased after Mid-T Heat Treatment

before mid-T heat treatment

instant heater shutdown

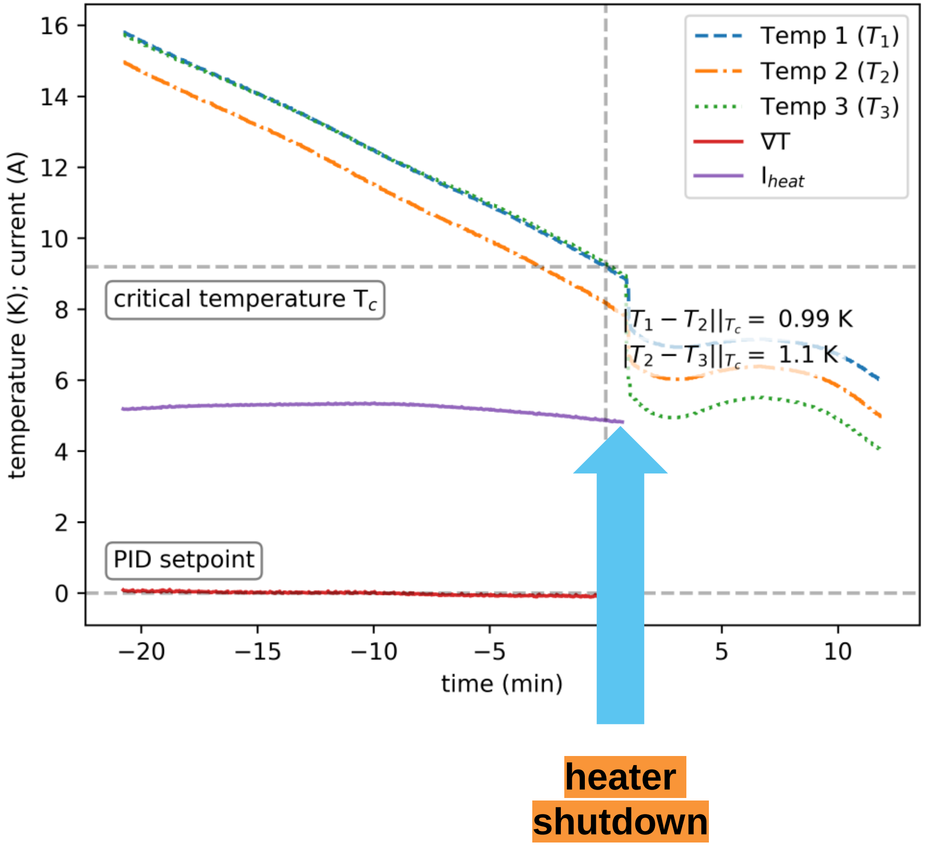

after mid-T heat treatment

soft heater shutdown

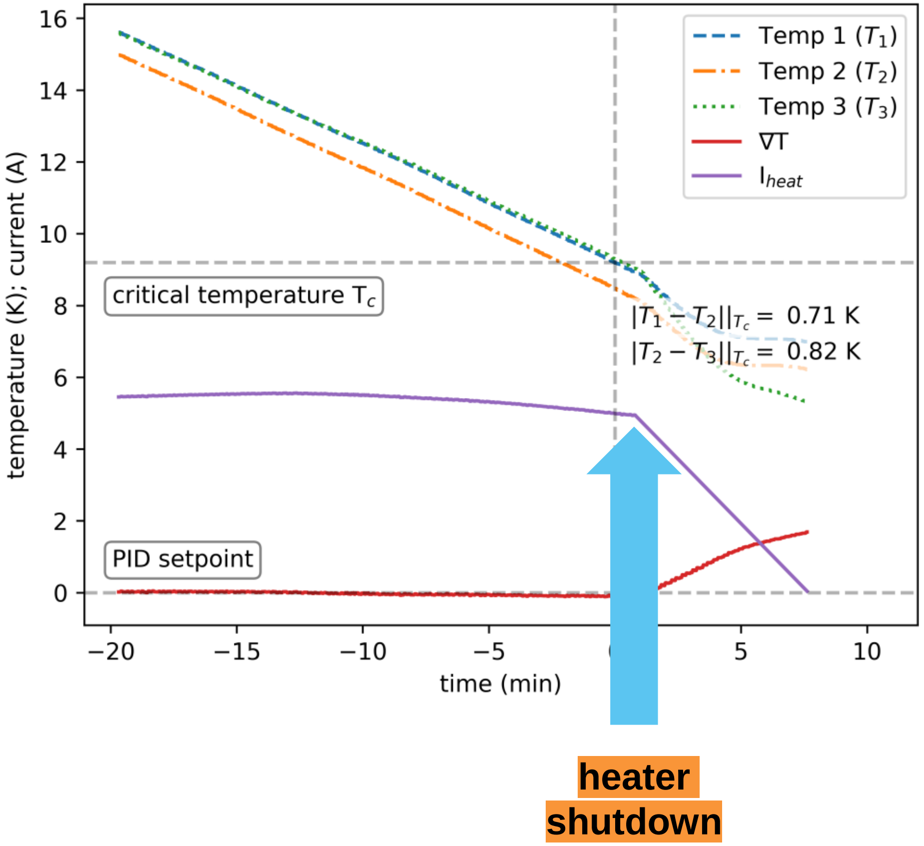

Results: Impact of Heater Shutdown Procedure on B_{sc} / B_{nc}

➢ <u>Contradictory</u> to Flux Expulsion Results: Real ∇T <u>Decreased</u> after Mid-T Heat Treatment

before mid-T heat treatment

instant heater shutdown

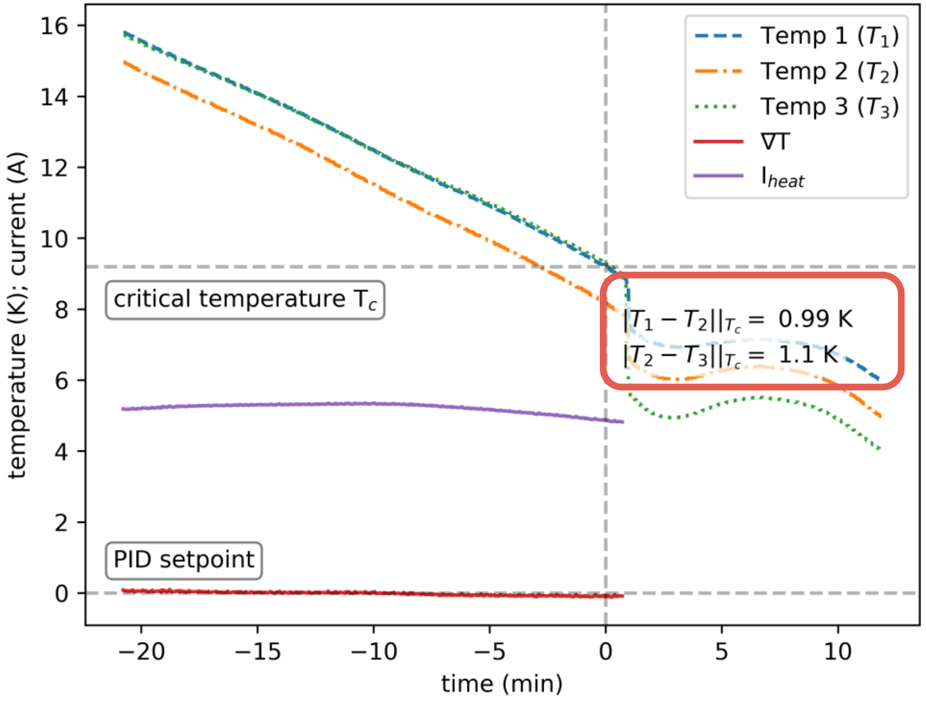

after mid-T heat treatment

soft heater shutdown

decrease of real ∇T

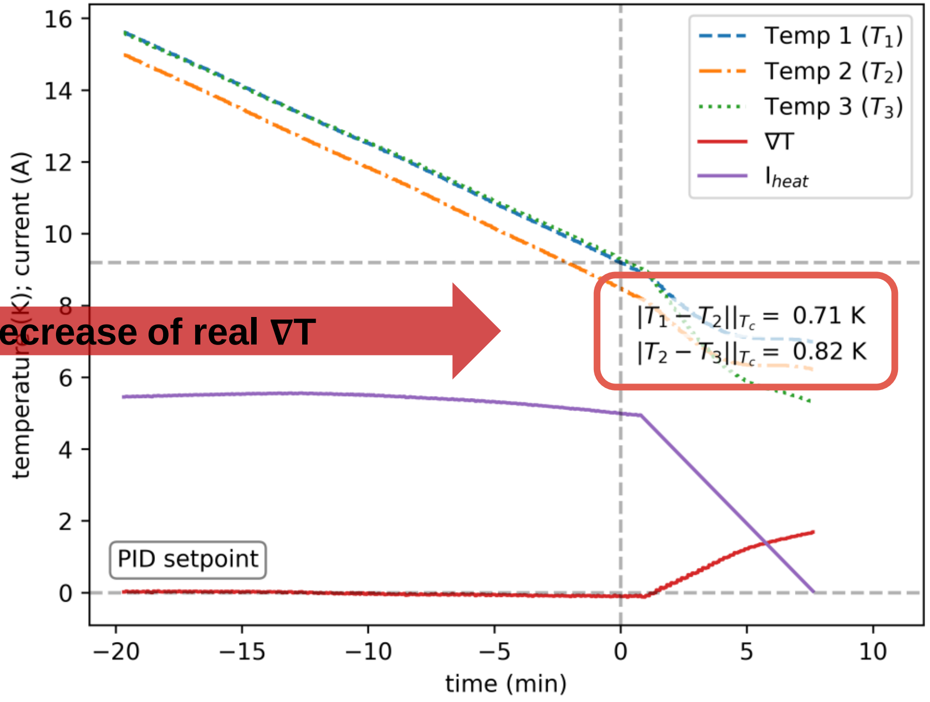

Results: Impact of Heater Shutdown Procedure on B_{sc} / B_{nc}

➢ **Measured Temperature Lower Than Surface Temperature**

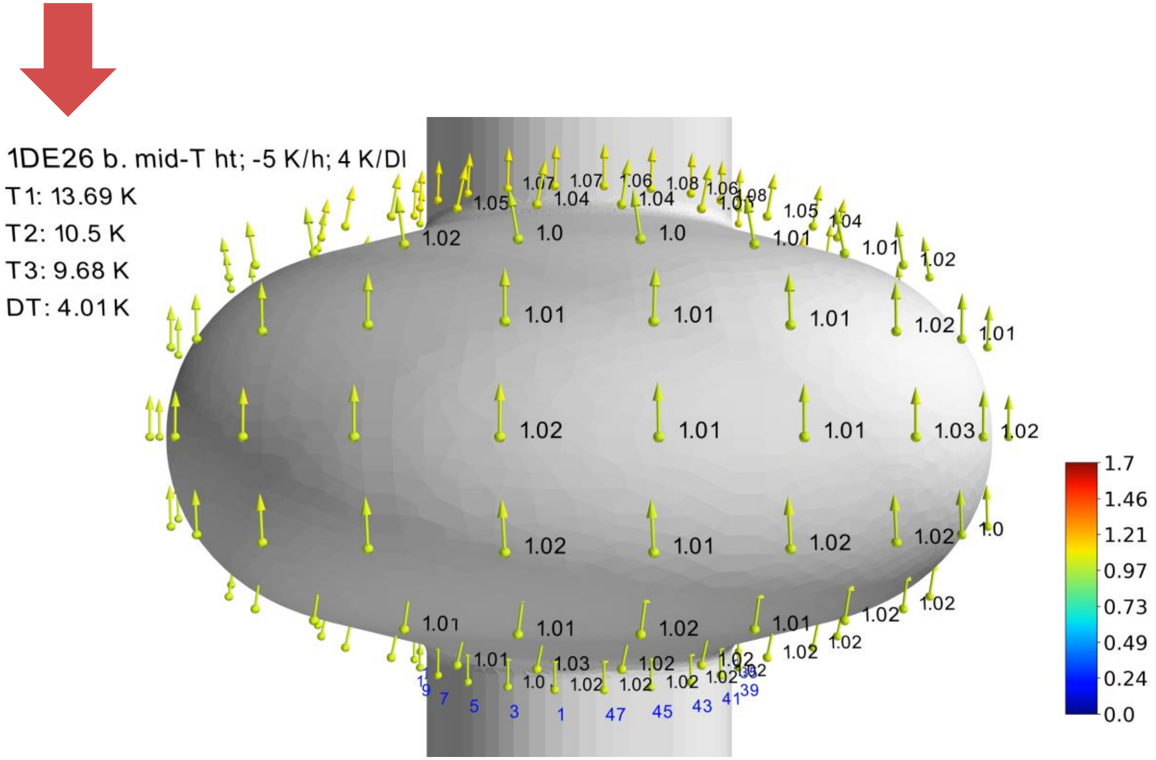

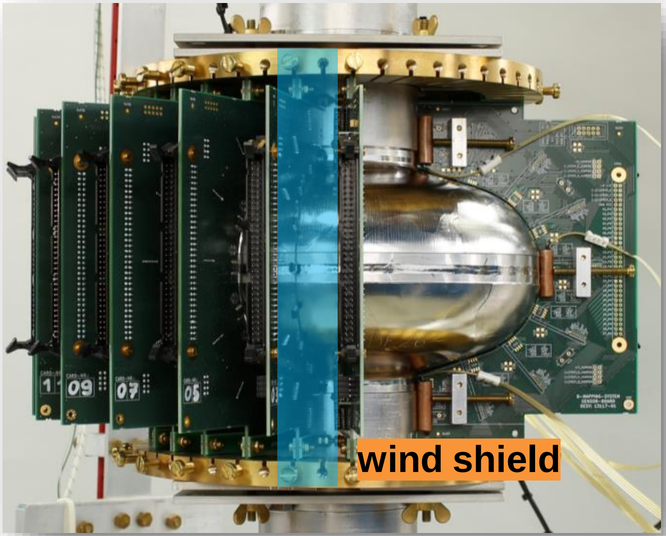

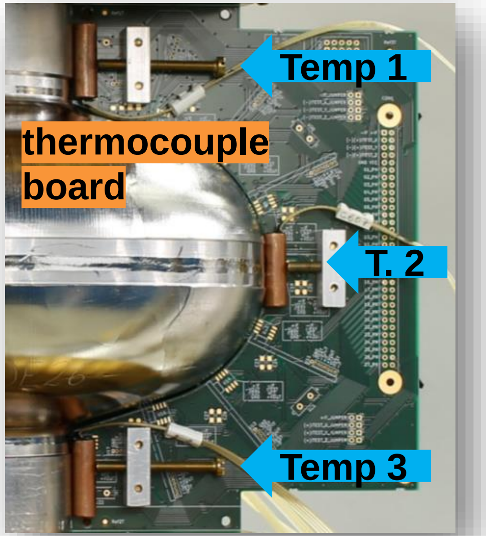

- ➢ thermocouples & holders exposed to helium gas flow due to missing wind shields
- ➢ surface temperature 2 - 3 K higher than measured temperature!

Results: Impact of Heater Shutdown Procedure on B_{sc} / B_{nc}

➢ **Cavity Partially Above T_c – Instant Heater Shutdown Results in Lower ∇T**

before mid-T heat treatment

instant heater shutdown

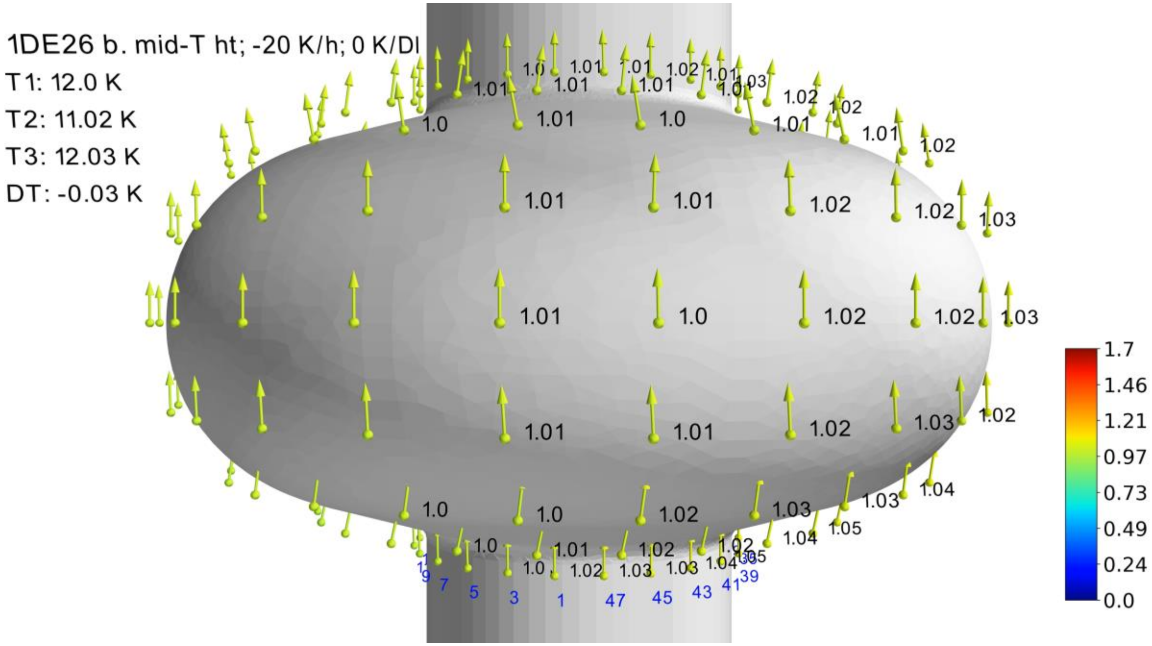

after mid-T heat treatment

soft heater shutdown

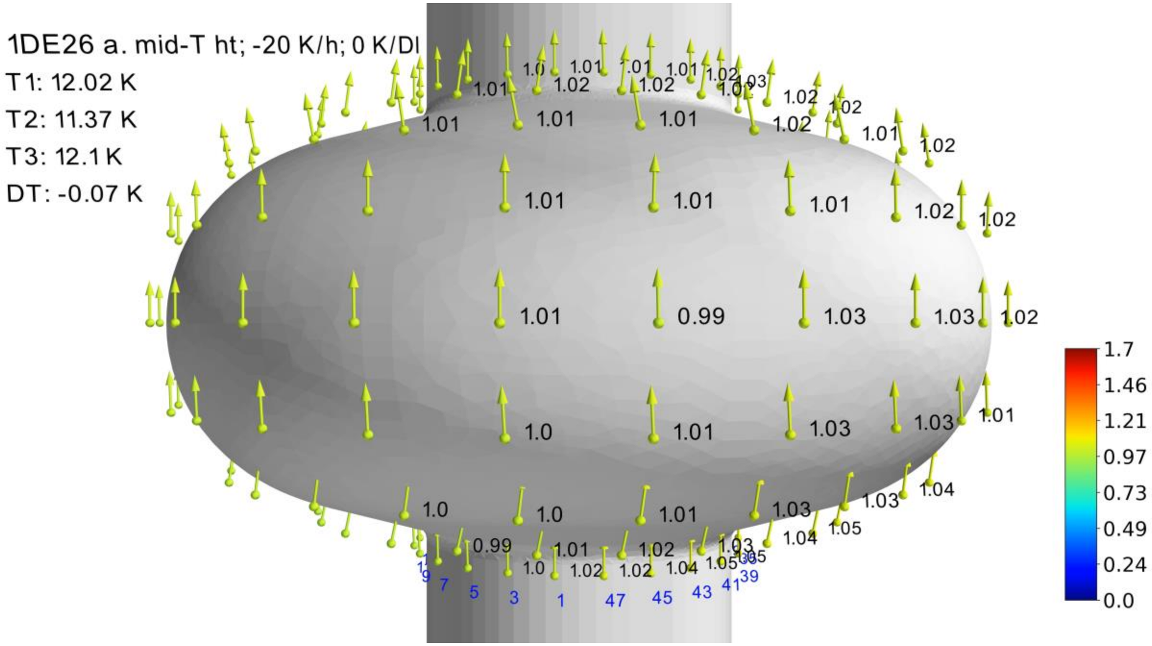

identical behavior until heater shutdown (T_1 = 8.9 K)

instant heater shutdown: lower ∇T

soft heater shutdown: larger ∇T → **increased flux expulsion**

Results: Impact of Heater Shutdown Procedure on B_{sc} / B_{nc}

➢ **Cavity Partially Above T_c – Instant Heater Shutdown Results in Lower ∇T**

before mid-T heat treatment (-20 K/h)
instant heater shutdown

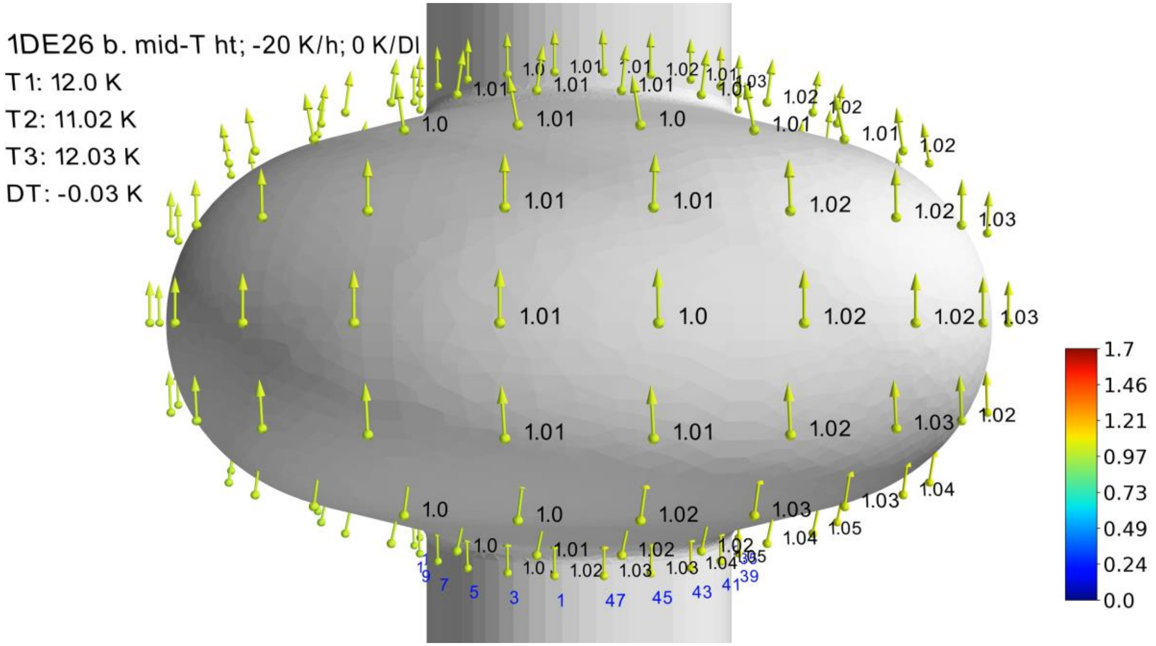

before mid-T heat treatment (-5 K/h)
soft heater shutdown

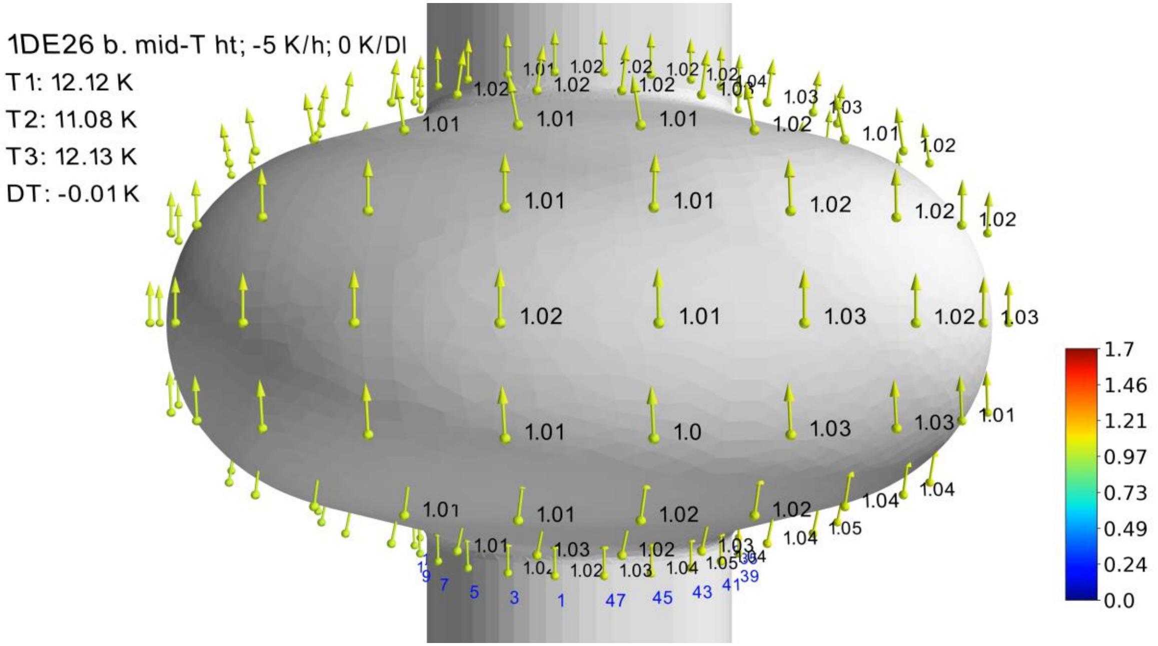

identical behavior until heater shutdown (T_1 = 8.9 K)

instant heater shutdown: lower ∇T

soft heater shutdown: larger ∇T → **increased flux expulsion**

Results: Impact of Mid-T Heat Treatment on B_{sc} / B_{nc}

➢ (Likely) No Impact of Mid-T Heat Treatment on Flux Expulsion Behavior

1DE03 fine-grain material
before mid-T heat treatment

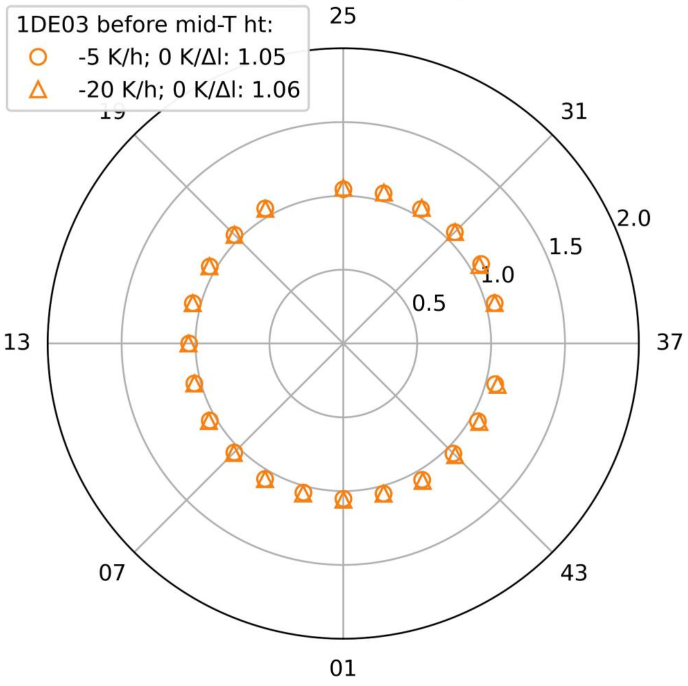

1DE09 fine-grain material
after mid-T heat treatment

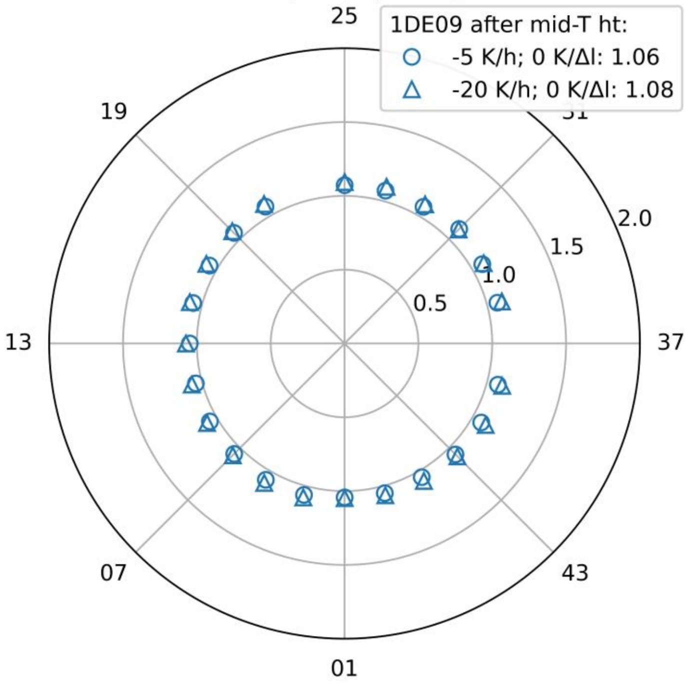

1DE26 large-grain material
before & after mid-T heat treatment

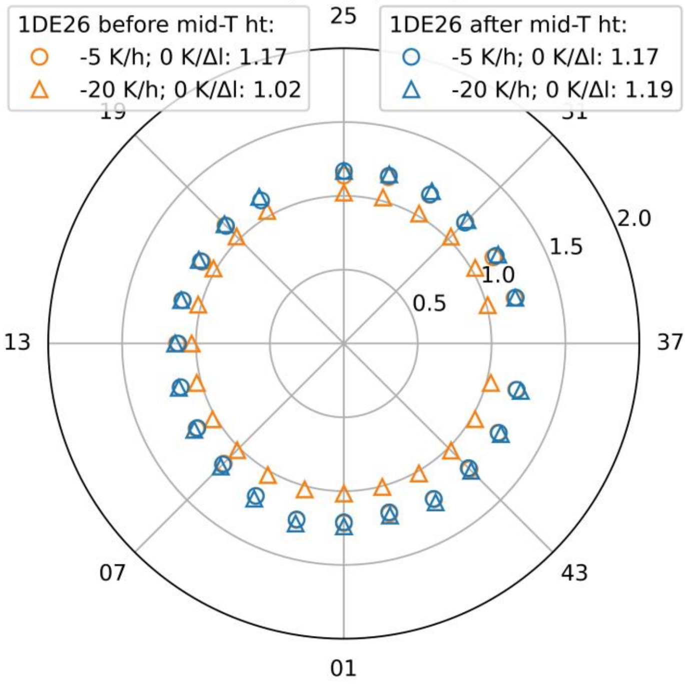

	1DE03 before	1DE03 after		1DE09 before	1DE09 after		1DE26 before	1DE26 after
-5 K/h; 0 K/ΔI:	90 %	- %	**-5 K/h; 0 K/ΔI:**	- %	88 %	**-5 K/h; 0 K/ΔI:**	68 %	68 %
-20 K/h; 0 K/ΔI:	89 %	- %	**-20 K/h; 0 K/ΔI:**	- %	84 %	**-20 K/h; 0 K/ΔI:**	(96 %)	64 %

Results: Impact of Spatial Temperature Gradient on B_{sc} / B_{nc}

➢ **Large Impact of Spatial Temperature Gradient on Flux Expulsion Behavior**

1DE03 fine-grain material
before mid-T heat treatment

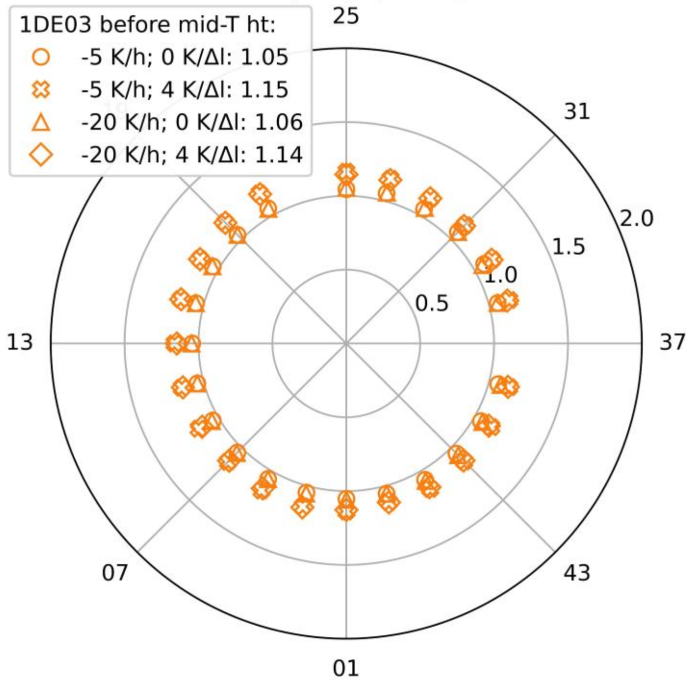

1DE09 fine-grain material
after mid-T heat treatment

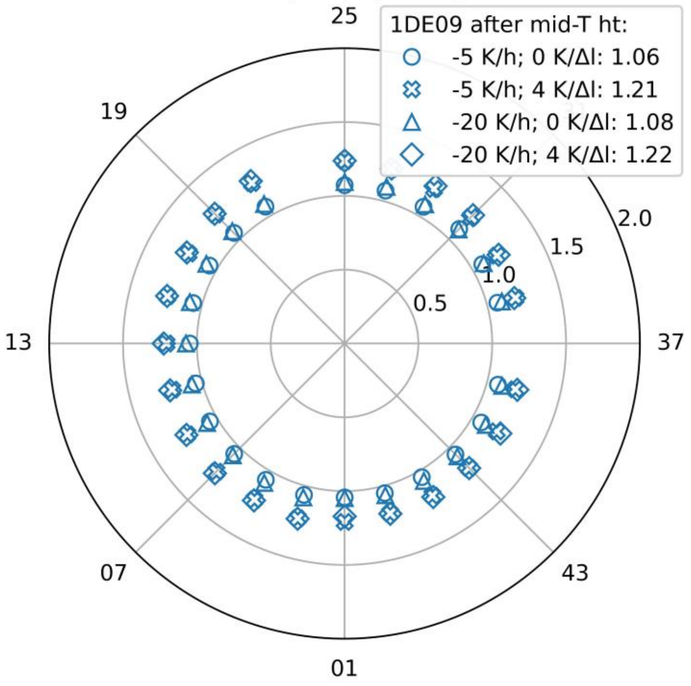

1DE26 large-grain material
before & after mid-T heat treatment

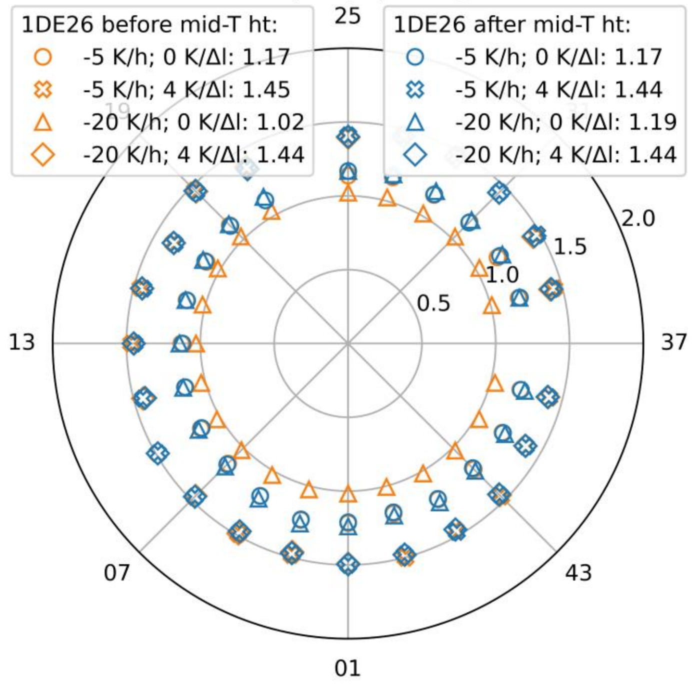

-5 K/h; 0 K/ΔI:	90 %	- %
-5 K/h; 4 K/ΔI:	73 %	- %
-20 K/h; 0 K/ΔI:	89 %	- %
-20 K/h; 4 K/ΔI:	74 %	- %

-5 K/h; 0 K/ΔI:	- %	88 %
-5 K/h; 4 K/ΔI:	- %	60 %
-20 K/h; 0 K/ΔI:	- %	84 %
-20 K/h; 4 K/ΔI:	- %	58 %

-5 K/h; 0 K/ΔI:	68 %	68 %
-5 K/h; 4 K/ΔI:	15 %	16 %
-20 K/h; 0 K/ΔI:	(96 %)	64 %
-20 K/h; 4 K/ΔI:	17 %	17 %

Results: Impact of Spatial Temperature Gradient on B_{sc} / B_{nc}

➢ **Large Impact of Spatial Temperature Gradient on Flux Expulsion Behavior**

1DE03 fine-grain material
before mid-T heat treatment

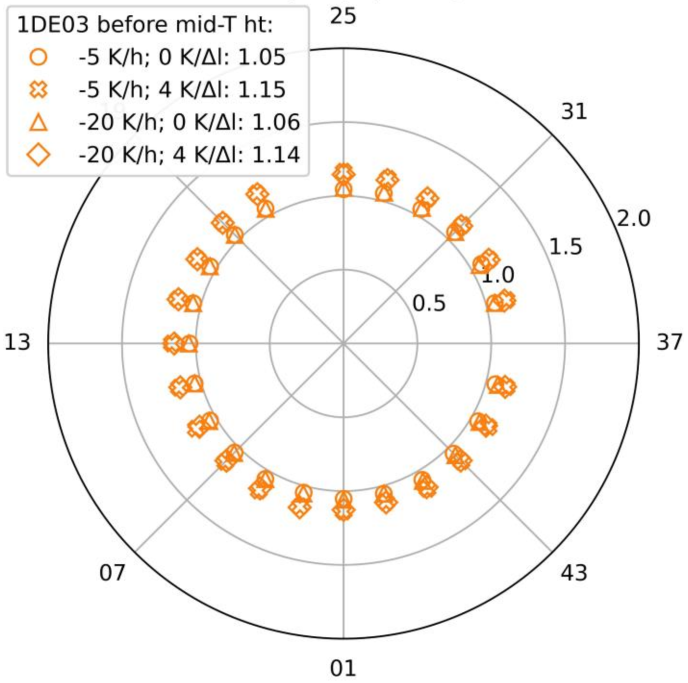

-5 K/h; 0 K/ΔI:	90 %	- %
-5 K/h; 4 K/ΔI:	73 %	- %
-20 K/h; 0 K/ΔI:	89 %	- %
-20 K/h; 4 K/ΔI:	74 %	- %

1DE09 fine-grain material
after mid-T heat treatment

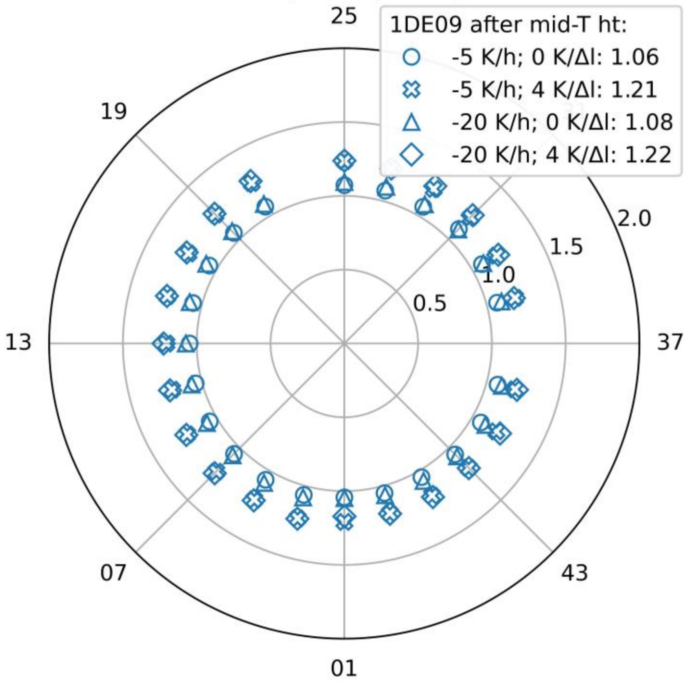

-5 K/h; 0 K/ΔI:	- %	88 %
-5 K/h; 4 K/ΔI:	- %	60 %
-20 K/h; 0 K/ΔI:	- %	84 %
-20 K/h; 4 K/ΔI:	- %	58 %

1DE26 large-grain material
before & after mid-T heat treatment

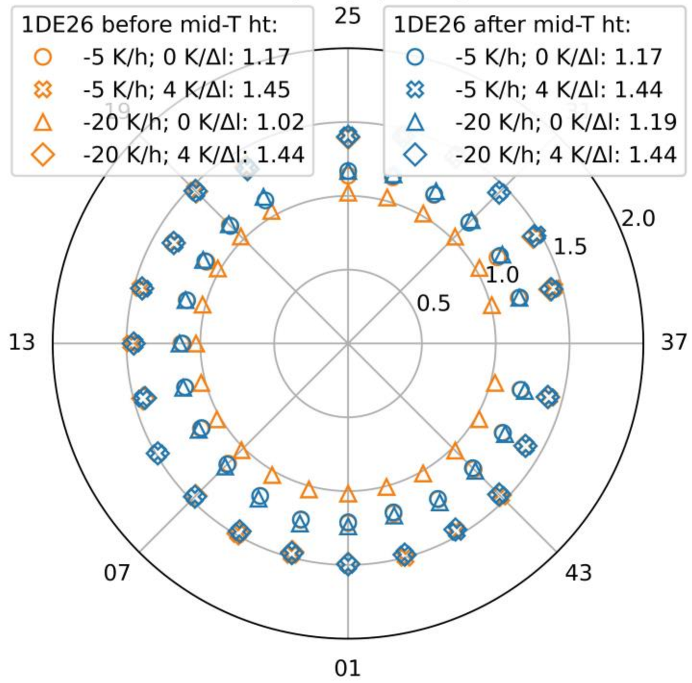

-5 K/h; 0 K/ΔI:	68 %	68 %
-5 K/h; 4 K/ΔI:	15 %	16 %
-20 K/h; 0 K/ΔI:	(96 %)	64 %
-20 K/h; 4 K/ΔI:	17 %	17 %

Results: Impact of Mid-T Heat Treatment on S

➢ **1DE26: Five Times Larger Sensitivity to Trapped Magnetic Flux S after Mid-T Heat Treatment**

1DE03 fine g.	fr. trapped	
-5 K/h; 0 K/ΔI:	90 %	
-5 K/h; 4 K/ΔI:	73 %	
-20 K/h; 0 K/ΔI:	89 %	
-20 K/h; 4 K/ΔI:	74 %	

1DE09 fine g.		fr. trapped
-5 K/h; 0 K/ΔI:		88 %
-5 K/h; 4 K/ΔI:		60 %
-20 K/h; 0 K/ΔI:		84 %
-20 K/h; 4 K/ΔI:		58 %

1DE26 large g.	fr. trapped	fr. trapped
-5 K/h; 0 K/ΔI:	68 %	68 %
-5 K/h; 4 K/ΔI:	15 %	16 %
-20 K/h; 0 K/ΔI:	(96 %)	64 %
-20 K/h; 4 K/ΔI:	17 %	17 %

Results: Impact of Mid-T Heat Treatment on S

➢ **1DE26: Five Times Larger Sensitivity to Trapped Magnetic Flux S after Mid-T Heat Treatment**

1DE03 fine g.	fr. trapped
-5 K/h; 0 K/ΔI:	90 %
-5 K/h; 4 K/ΔI:	73 %
-20 K/h; 0 K/ΔI:	89 %
-20 K/h; 4 K/ΔI:	74 %

1DE09 fine g.	fr. trapped
-5 K/h; 0 K/ΔI:	88 %
-5 K/h; 4 K/ΔI:	60 %
-20 K/h; 0 K/ΔI:	84 %
-20 K/h; 4 K/ΔI:	58 %

1DE26 large g.	fr. trapped	fr. trapped
-5 K/h; 0 K/ΔI:	68 %	68 %
-5 K/h; 4 K/ΔI:	15 %	16 %
-20 K/h; 0 K/ΔI:	(96 %)	64 %
-20 K/h; 4 K/ΔI:	17 %	17 %

obtain R_s

- ➢ record QE curve
- ➢ calculate $R_s = G/Q_0$
- ➢ interpolate $R_s(4\,MV/m)$

approximate R_{flux}

- ➢ $R_s = R_{res} + R_{BCS} + R_{flux}$
- ➢ $R_{s\_baseline} = R_{res} + R_{BCS}$
- ➢ $R_{flux} = R_s - R_{s\_baseline}$

Results: Impact of Mid-T Heat Treatment on S

➢ **1DE26: Five Times Larger Sensitivity to Trapped Magnetic Flux S after Mid-T Heat Treatment**

1DE03 fine g.	fr. trapped	R_s (nΩ)	R_{flux} (nΩ)	S (nΩ/μT)
-5 K/h; 0 K/Δl:	90 %	50.1	38.1	4.2
-5 K/h; 4 K/Δl:	73 %	38.9	26.9	3.7
-20 K/h; 0 K/Δl:	89 %	49.8	37.7	4.2
-20 K/h; 4 K/Δl:	74 %	39.7	27.7	3.7

1DE09 fine g.	fr. trapped	R_s (nΩ)	R_{flux} (nΩ)	S (nΩ/μT)
-5 K/h; 0 K/Δl:	88 %	166.5	159.4	18.1
-5 K/h; 4 K/Δl:	60 %	96.5	89.3	15.0
-20 K/h; 0 K/Δl:	84 %	158.9	151.8	18.0
-20 K/h; 4 K/Δl:	58 %	95.3	88.2	15.2

sensitivity to trapped magnetic flux S [H. Ito et al.]:
$S = R_{flux} / B_{trap}$

1DE26 large g.	fr. trapped	R_s (nΩ)	R_{flux} (nΩ)	bef. mid-T S (nΩ/μT)	fr. trapped	R_s (nΩ)	R_{flux} (nΩ)	aft. mid-T S (nΩ/μT)
-5 K/h; 0 K/Δl:	68 %	37.9	26.1	3.8	68 %	137.8	130.7	19.3
-5 K/h; 4 K/Δl:	15 %	21.4	9.6	6.5	16 %	[illegible]	49.0	30.4
-20 K/h; 0 K/Δl:	(96 %)	(52.6)	(40.8)	4.3	64 %	130.6	123.4	19.3
-20 K/h; 4 K/Δl:	17 %	21.9	10.1	6.0	17 %	56.0	48.8	29.2

5 x

Results: Impact of Mid-T Heat Treatment on S

➢ 1DE26: Five Times Larger Sensitivity to Trapped Magnetic Flux S after Mid-T Heat Treatment

1DE03 fine g.	fr. trapped	R_s (nΩ)	R_{flux} (nΩ)	bef. mid-T S (nΩ/µT)
-5 K/h; 0 K/ΔI:	90 %	50.1	38.1	4.2
-5 K/h; 4 K/ΔI:	73 %	38.9	26.9	3.7
-20 K/h; 0 K/ΔI:	89 %	49.8	37.7	4.2
-20 K/h; 4 K/ΔI:	74 %	39.7	27.7	3.7

4 x

1DE09 fine g.	fr. trapped	R_s (nΩ)	R_{flux} (nΩ)	aft. mid-T S (nΩ/µT)
-5 K/h; 0 K/ΔI:	88 %	166.5	159.4	18.1
-5 K/h; 4 K/ΔI:	60 %	96.5	89.3	15.0
-20 K/h; 0 K/ΔI:	84 %	158.9	151.8	18.0
-20 K/h; 4 K/ΔI:	58 %	95.3	88.2	15.2

sensitivity to trapped magnetic flux S [H. Ito et al.]:
$S = R_{flux} / B_{trap}$

1DE26 large g.	fr. trapped	R_s (nΩ)	R_{flux} (nΩ)	bef. mid-T S (nΩ/µT)	fr. trapped	R_s (nΩ)	R_{flux} (nΩ)	aft. mid-T S (nΩ/µT)
-5 K/h; 0 K/ΔI:	68 %	37.9	26.1	3.8	68 %	137.8	130.7	19.3
-5 K/h; 4 K/ΔI:	15 %	21.4	9.6	6.5	16 %	56.1	49.0	30.4
-20 K/h; 0 K/ΔI:	(96 %)	(52.6)	(40.8)	4.3	64 %	130.6	123.4	19.3
-20 K/h; 4 K/ΔI:	17 %	21.9	10.1	6.0	17 %	56.0	48.8	29.2

5 x

Take Home Messages

accurate simulations of ideal Meissner state possible:

- detailed simulation model
- high mesh resolution

flux expulsion behavior (for used conditions):

- no significant impact of cool down velocity
- large impact of spatial temperature gradient

mid-T heat treatment:

- no impact of mid-T heat treatment on flux expulsion behavior
- five times larger sensitivity to trapped magnetic flux after mid-T heat treatment

Thank You For Your Attention!

We would like to thank our colleagues – A. Miyazaki from Universite Paris-Saclay, F. Kramer and O. Kugeler from Helmholtz-Zentrum Berlin, I. Flick, R. Ghanbari, I. Gonzalez Diaz-Palacio, S. Harder, G. Kacha Deyu, C. Saribal and M. Wenskat from University of Hamburg as well as the DESY groups MDI, MKS1, MSL and ZE - for their support of this work.

References

[B. Schmitz et al.] B. Schmitz, J. Köszegi, K. Alomari, O. Kugeler, and J. Knobloch, “Magnetometric Mapping of Superconducting RF Cavities,” Rev. Sci. Instrum., vol. 89, 2018. doi:10.1063/1.5030509

[F. Kramer et al.] F. Kramer, O. Kugeler, J.-M. Köszegi, and J. Knobloch, “Impact of geometry on flux trapping and the related surface resistance in a superconducting cavity,” Phys. Rev. Accel. Beams, vol. 23, no. 12, p. 123 101, 2020. doi:10.1103/PhysRevAccelBeams.23.123101

[F. Kramer et al. 22] F. Kramer, S. Keckert, J. Knobloch, and O. Kugeler, “Systematic Investigation of Flux Trapping Dynamics in Niobium Samples,” in Proc. IPAC’22, Bangkok, Thailand, 2022, pp. 1200–1203. doi:10.18429/JACoW-IPAC2022-TUPOTK006

[H. Ito et al.] H. Ito, H. Araki, K. Takahashi, and K. Umemori, “Influence of furnace baking on Q–E behavior of superconducting accelerating cavities,” Prog. Theor. Exp. Phys., vol. 2021, no. 7, 2021, 071G01. doi:10.1093/ptep/ptab056